

TECHNO-FUNCTIONAL PROPERTIES OF HIGH PROTEIN EXTRUDATES
OBTAINED BY LOW AND HIGH MOISTURE EXTRUSION PROCESS

A THESIS SUBMITTED TO
THE GRADUATE SCHOOL OF NATURAL AND APPLIED SCIENCES
OF
MIDDLE EAST TECHNICAL UNIVERSITY



BY

İLHAN ÇALIŞKAN

IN PARTIAL FULFILLMENT OF THE REQUIREMENTS
FOR
THE DEGREE OF MASTER OF SCIENCE
IN
FOOD ENGINEERING

DECEMBER 2024

Approval of the thesis:

**TECHNO-FUNCTIONAL PROPERTIES OF HIGH PROTEIN
EXTRUDATES OBTAINED BY LOW AND HIGH MOISTURE
EXTRUSION PROCESS**

submitted by **İLHAN ÇALIŞKAN** in partial fulfillment of the requirements for the degree of **Master of Science in Food Engineering, Middle East Technical University** by,

Prof. Dr. Naci Emre ALTUN
Dean, **Graduate School of Natural and Applied Sciences**

Prof. Dr. Hami Alpas
Head of the Department, **Food Engineering**

Prof. Dr. İlkay Şensoy
Supervisor, **Food Engineering, METU**

Prof. Dr. Behiç Mert
Co-Supervisor, **Food Engineering, METU**

Examining Committee Members:

Prof. Dr. Yeşim Soyer Küçükşenel
Food Engineering, METU

Prof. Dr. İlkay Şensoy
Food Engineering, METU

Prof. Dr. Behiç Mert
Food Engineering, METU

Assoc. Prof. Dr. Özge Şakıyan Demirkol
Food Engineering, Ankara University

Assoc. Prof. Dr. Leyla N. Kahyaoğlu
Food Engineering, METU

Date: 02.12.2024



I hereby declare that all information in this document has been obtained and presented in accordance with academic rules and ethical conduct. I also declare that, as required by these rules and conduct, I have fully cited and referenced all material and results that are not original to this work.

Name Last name : İlhan Çalışkan

Signature :

ABSTRACT

TECHNO-FUNCTIONAL PROPERTIES OF HIGH PROTEIN EXTRUDATES OBTAINED BY LOW AND HIGH MOISTURE EXTRUSION PROCESS

Çalışkan, İlhan
Master of Science, Food Engineering
Supervisor : Prof. Dr. İlkay Şensoy
Co-Supervisor: Prof. Dr. Behiç Mert

December 2024, 57 pages

Hemp seed protein has a potential as an alternative protein source to wheat and soy proteins, due to its high nutritional content and non-allergenicity. This study aimed to investigate the use of hemp flour, a by-product of oil extraction, in the production of meat analogues, using both low and high moisture extrusion techniques. During the low moisture extrusion, the hemp flour (H) and gluten flour (G) in the ratio of 60:40 (H:G, g:g dry weight) were extruded with three different moisture levels (20%, 30%, and 40%) at two different barrel temperature profiles (60°C, 70°C, 100°C, 120°C, and 60°C, 70°C, 100°C, 150°C). In the high moisture extrusion, hemp flour was mixed with soy protein isolate (SPI) in three different ratios (H:SPI, g:g dry weight): 0:100, 25:75, and 50:50, then extruded at three different moisture levels (65%, 70%, and 75%) and two different barrel temperature profiles (40°C, 60°C, 80°C, 100°C, and 60°C, 80°C, 100°C, 125°C). Techno-functional properties, colour and textural properties of extruded products were examined. The findings indicated that low moisture meat analogues could be effectively produced using a 60:40 ratio of H to G. Moreover, the results highlighted the potential for generating high-quality fibrous high moisture meat analogues that mimic the textural characteristics of

chicken breast by blending H with SPI up to 50:50 ratio. In summary, this study underscores the promise of hemp flour as a significant protein source for developing innovative extruded products. Future investigations may concentrate on sensory attributes to develop consumer-friendly meat analogues utilizing hemp flour.

Keywords: Meat analogue, Hemp meal, Plant protein



ÖZ

DÜŞÜK VE YÜKSEK NEMLİ EKSTRÜZYON YÖNTEMİYLE ELDE EDİLEN YÜKSEK PROTEİNLİ EKSTÜDELERİN TEKNO-FONKSİYONEL ÖZELLİKLERİNİN BELİRLENMESİ

Çalışkan, İlhan
Yüksek Lisans, Gıda Mühendisliği
Tez Yöneticisi: Prof. Dr. İlkay Şensoy
Ortak Tez Yöneticisi: Prof. Dr. Behiç Mert

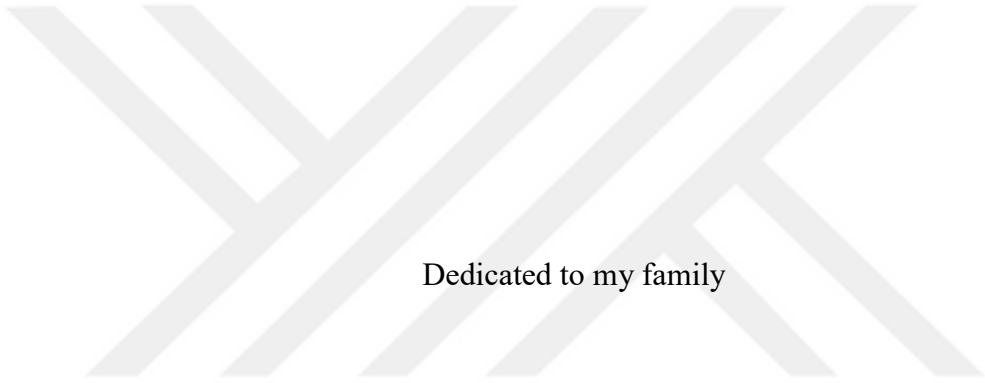
Aralık 2024, 57 sayfa

Kenevir tohumu proteini, yüksek besin içeriği ve alerjen olmaması nedeniyle buğday ve soya proteinlerine alternatif bir protein kaynağı olma potansiyele sahiptir. Bu çalışma, yağ ekstraksiyonunun bir yan ürünü olan kenevir ununun hem düşük hem de yüksek nemli ekstrüzyon teknikleri kullanılarak et analogu üretiminde kullanımını araştırmayı amaçlamıştır. Düşük nemli ekstrüzyonu sırasında, kenevir unu (K) ve gluten unu (G) 60:40 oranında (K:G, g:g kuru baz), iki farklı sıcaklık profili (60°C, 70°C, 100°C, 120°C ve 60°C, 70°C, 100°C, 150°C) ile üç farklı nem seviyesinde (20%, 30% ve 40%) ekstrüde edilmiştir. Yüksek nemli ekstrüzyonda ise, kenevir unu soya protein izolatu (SPI) ile üç farklı oranda (K:SPI, g:g kuru baz), karıştırıldı: 0:100, 25:75 ve 50:50, sonra üç farklı nem içeriğinde (%65 %70 ve %75) ve iki farklı sıcaklık profiliyle (40°C, 60°C, 80°C, 100°C ve 60°C, 80°C, 100°C, 125°C) ekstrüzyon işleminden geçirildi. Ekstrüde ürünlerin tekno-fonksiyonel özellikleri, renk ve tekstür özellikleri incelendi. Bulgular, düşük nemli et analoglarının 60:40 oranında K ve G kullanılarak etkili bir şekilde üretilebileceğini gösterdi. Ayrıca sonuçlar K'nın SPI ile 50:50 oranında karıştırılarak tavuk göğsünün tekstür özelliklerini taklit edebilen yüksek kalitede lifli, yüksek nemli et analogu

retme potansiyelini gstermiřtir. zetle, bu alıřma, yeniliki ekstrde rnler geliřtirmek iin nemli bir protein kaynađı olarak kenevir ununun potansiyelini vurgulamaktadır. Gelecek arařtırmalar, kenevir unuyla tketicici dostu et analog geliřtirmek amacıyla duyuusal zelliklere odaklanabilir.

Anahtar Kelimeler: Et analog, Kenevir unu, Bitkisel protein





Dedicated to my family

ACKNOWLEDGMENTS

First and foremost, I am extremely grateful to my advisor, Prof. Dr. İlkey Şensoy, for her constant support, guidance, and contribution during my study.

I would also like to express my thanks to my Co-advisor Prof. Dr. Behiç Mert for his assistive guidance and support.

I would like to extend my thanks to Dr. Özge Güven for his support and contribution throughout my study.

Besides, I would like to express my gratitude to my laboratory mates Ms. Deniz Günelan, Ms. Elif Kahvecioğlu, and Ms. Elifsu Polat.

From the bottom of my heart, I would like to express my gratitude to my beloved wife, Esra Çalışkan, my son Mustafa Kaan Çalışkan, and my daughter İpek Çalışkan for their support, encouragement, and patience at all stages during my study.

This work was supported by the Scientific and Technological Research Council of Turkey (TÜBİTAK-1220790) and METU Scientific Research Projects Coordination Unit (TEZ-D-314-2021-10703).

TABLE OF CONTENTS

ABSTRACT.....	v
ÖZ	vii
ACKNOWLEDGMENTS	x
TABLE OF CONTENTS.....	xi
LIST OF TABLES	xiii
LIST OF FIGURES	xiv
LIST OF ABBREVIATIONS.....	xvi
1 INTRODUCTION	1
1.1 Meat Analogues.....	1
1.2 Extrusion Technology	3
1.3 Plant Proteins.....	5
1.4 Hemp	6
2 MATERIALS AND METHODS.....	9
2.1 Materials.....	9
2.2 Methods.....	9
2.2.1 Low Moisture Extrusion	10
2.2.1.1 Bulk Density	11
2.2.1.2 Water Absorption Index (WAI) and Water Solubility Index (WSI)	11
2.2.1.3 Oil Absorption Index (OAI)	12
2.2.1.4 Water Holding Capacity (WHC)	13
2.2.1.5 Integrity Index	13
2.2.1.6 Colour Measurements	14

2.2.1.7	Texture Profile Analyses (TPA).....	14
2.2.2	High Moisture Extrusion	15
2.2.2.1	Colour Measurements	16
2.2.2.2	Texture Profile Analyses (TPA) and Degree of Texturization ..	16
2.2.3	Statistical Analyses.....	18
3	RESULTS AND DISCUSSION.....	19
3.1.1	Low Moisture Extrusion.....	19
3.1.1.1	Physical properties	19
3.1.1.2	Colour.....	25
3.1.1.3	Texture Profile Analyses (TPA).....	26
3.1.2	High Moisture Extrusion	29
3.1.2.1	Colour.....	29
3.1.2.2	Texture Profile Analyses (TPA) and Degree of Texturization ..	33
4	CONCLUSION AND RECOMMENDATIONS	39
	REFERENCES	41
A.	Moisture data of HMMA samples.....	51
B.	Images of LMMA extrudates	52
C.	Images of HMMA extrudates.....	53

LIST OF TABLES

TABLES

Table 1: Amino acid composition (g/100 g) of hemp protein isolate (HPI), hemp protein concentrate (HPC), soy protein isolate (SPI), red meat and chicken breast .	7
Table 2: Compositions of the flours as specified by the companies	9
Table 3: Screw configurations of the extruder.....	10
Table 4: Physical Properties of LMMAAs extruded at different moisture levels and temperatures profiles.....	24
Table 5: Colour parameters of LMMA samples extruded at different moisture levels and temperature profiles	26
Table 6: Hardness values of dry LMMA samples extruded at different temperature profiles	27
Table 7: Textural properties of hydrated LMMA samples extruded at different temperature profiles	28
Table 8: Colour parameters of HMMA samples extruded at different moisture and temperature profiles	32
Table 9: Textural properties of HMMA samples extruded at different moisture level and temperature profiles.....	36
Table 10: Degree of texturization of HMMAAs with different H:SPI ratios produced at different moisture content and temperature profiles	37

LIST OF FIGURES

FIGURES

Figure 1: Images of LMMA samples extruded at different moisture level and temperature profiles	20
Figure 2: Images of HMMA samples extruded at lower temperature profile (last zone temperature of 100 °C) for different moisture and hemp addition levels	30
Figure 3: Images of HMMA samples extruded at higher temperature profile (last zone temperature of 125 °C) for different moisture and hemp addition levels	31
Figure 4: LMMA, H:G_60:40, 20% moisture, 120°C.....	52
Figure 5: LMMA, H:G_60:40, 20% moisture, 150°C.....	52
Figure 6: HMMA, H:SPI_0:100, 65% moisture, 100°C. Images of surface, longitudinal to flow and transversal to flow, respectively	53
Figure 7: HMMA, H:SPI_0:100, 70% moisture, 100°C. Images of surface, longitudinal to flow and transversal to flow, respectively	53
Figure 8: HMMA, H:SPI_0:100, 75% moisture, 100°C. Images of surface, longitudinal to flow and transversal to flow, respectively	53
Figure 9: HMMA, H:SPI_25:75, 65% moisture, 100°C. Images of surface, longitudinal to flow and transversal to flow, respectively	54
Figure 10: HMMA, H:SPI_25:75, 70% moisture, 100°C. Images of surface, longitudinal to flow and transversal to flow, respectively	54
Figure 11: HMMA, H:SPI_25:75, 75% moisture, 100°C. Images of surface, longitudinal to flow and transversal to flow, respectively	54
Figure 12: HMMA, H:SPI_50:50, 65% moisture, 100°C. Images of surface, longitudinal to flow and transversal to flow, respectively	55
Figure 13: HMMA, H:SPI_50:50, 70% moisture, 100°C. Images of surface, longitudinal to flow and transversal to flow, respectively	55
Figure 14: HMMA, H:SPI_50:50, 75% moisture, 100°C. Images of surface, longitudinal to flow and transversal to flow, respectively	55
Figure 15: HMMA, H:SPI_0:100, 65% moisture, 125°C. Images of surface, longitudinal to flow and transversal to flow, respectively	56

Figure 16: HMMA, H:SPI_0:100, 70% moisture, 125°C. Images of surface, longitudinal to flow and transversal to flow, respectively	56
Figure 17: HMMA, H:SPI_0:100, 75% moisture, 125°C. Images of surface, longitudinal to flow and transversal to flow, respectively	56
Figure 18: HMMA, H:SPI_25:75, 65% moisture, 125°C. Images of surface, longitudinal to flow and transversal to flow, respectively	57
Figure 19: HMMA, H:SPI_25:75, 70% moisture, 125°C. Images of surface, longitudinal to flow and transversal to flow, respectively	57
Figure 20: HMMA, H:SPI_50:50, 65% moisture, 125°C. Images of surface, longitudinal to flow and transversal to flow, respectively	57

LIST OF ABBREVIATIONS

G	Gluten Flour
LMMA	Low-Moisture Meat Analogues
H	Hemp Flour
HMMA	High-Moisture Meat Analogues
OAI	Oil Absorption Index
SPI	Soy Protein Isolate
TPA	Texture Profile Analyses
WAI	Water Absorption Index
WHC	Water Holding Capacity
WSI	Water Solubility Index

CHAPTER 1

INTRODUCTION

Meat is a widely consumed food due to its appealing texture, good nutritional quality, and its association with social status particularly in Western countries (Shaghaghian et al., 2022). However, consuming processed red meat has been associated with health risks, specifically in relation to cancer, coronary heart disease, and cardiovascular disorders. Another disadvantage of conventional red meat production is its detrimental effects on the environment. Reducing or eliminating animal-based foods from the diet can result in substantial reductions in land usage, water requirements, and greenhouse gas emissions (Herz et al., 2021).

In order to provide adequate food production for the projected world population by 2050, significant changes are needed in industry and society regarding continuous food manufacturing (Mateen et al., 2023a). From this point of view, the expected socioeconomic and demographic shifts will result in an increased demand for novel high-protein foods (Dinani et al., 2023).

The growing knowledge of negative environmental effects of animal-origin foods has significantly contributed to the growing popularity of plant-based diets in modern world (Diaz et al., 2022). There are many ongoing researches on replacing animal-based products with plant-based foods and meat analogues. Meat analogues can be defined as food products produced from alternative protein sources and structured to show similar sensory characteristics to meat (Chiang et al., 2019).

1.1 Meat Analogues

The global population is growing rapidly, which means that meat production in the near future may not be able to keep up with the demand. Furthermore, the production

of animal meat is causing environmental issues such as greenhouse gas emissions, excessive use of agricultural land, and high water consumption (Lee et al., 2022). Consumers are increasingly interested in substituting meat proteins with proteins produced from non-animal sources due to shifts in perceptions of health, environmental impact and animal welfare (Webb et al., 2023).

The term "meat analogue" can be defined as food products that mimic the taste, look, nutrition content, and texture of meat, without containing animal meat (Sun et al., 2021). Meat analogues, produced from plant-based ingredients, can mimic traditional meat with low carbon emissions, making them a recommended alternative to meat (Shanmugam et al., 2023). Also, meat analogues produced from plant-based proteins can provide an alternative to meat appealing to consumers without sacrificing the meat texture and meat flavour that they are accustomed to (Webb et al., 2023).

Meat proteins generally comprise all the essential amino acids necessary for humans in a form that the body can easily use. Therefore, it's crucial for the plant-based food industry to focus not only on creating products that imitate the taste and texture of real meat, but also on ensuring that the nutritional qualities of meat alternatives are the same as or better than those offered by real meat (Shaghaghian et al., 2022).

Extensive studies within the field of food science and technology have focused on the process of combining two or more ingredients to produce a superior product that exhibits the qualities of all its constituents. Currently, plant-based meat analogues are primarily produced from soybeans, which is the third-largest crop in the world after wheat and rice; however, soy crops are mostly genetically modified and may cause allergies (Lee et al., 2023a). The use of soy protein concentrates and isolates, along with wheat gluten, is common in producing meat analogues through extrusion. Their wide use is due to their convenient gelling properties and the potential to form a fibrous matrix structure. Endeavors are currently focused on finding a sustainable alternatives for use in meat analogue production (Zahari et al., 2023).

It is essential to investigate plants that can be a new protein source for the production of meat analogues. Additionally, exploring new plant protein sources is essential to broaden the range of ingredients for making meat analogues (Lee et al., 2022)

Currently, whole meat analogues made from plant proteins are created using various technologies and equipment, including extruders having cooling features, electrospinning, and shear cell technology. Among these, the twin-screw extruder with a cooling die appears to be the most promising for short-term scale-up (Mateen et al., 2023a).

1.2 Extrusion Technology

The term “extrusion” comes from the Latin word “extrude,” meaning “thrust out” or “force out.” Extrusion is a process where a material, such as metal, plastic, or a blend of food ingredients, is forced through a specific-shaped exit or aperture under high temperature and pressure (Prabha et al., 2021). Food extrusion process involves forcing ingredients to flow through a barrel while undergoing thermal and mechanical treatment and then pushing them through a specifically shaped exit or aperture to obtain various food products. While inside the barrel, the ingredients undergo compression, kneading, mixing, shearing, and high-temperature cooking, transforming them into a molten fluid. This molten substance is then forced through a die to produce semi or fully-cooked food with minimum loss of nutrients (Prabha et al., 2021).

In a simplified system analysis model, extrusion parameters are divided into three main groups: process, system, and product parameters. Examples of some process parameters are raw material formulation, screw components arrangement die dimensions, screw speed, moisture content, and barrel temperature (Mateen et al., 2023a). Parameters such as energy input, waiting time, molten substance temperature, molten substance pressure, and molten substance viscosity can be given

as examples of system parameters. Texture, colour, nutrition, taste, and digestibility of the final product are examples of product parameters (Mateen et al., 2023a).

There are two classes of extruded meat analogues based on the amount of water added during extrusion cooking: low moisture meat analogues with less than 35% water, high moisture meat analogues with higher than 50% water (Lee et al., 2022a).

Typically, low moisture extrusion produces textured proteins that have a significantly lower moisture content compared to high moisture extrusion (Zhang et al., 2024). In low moisture extrusion, the mixture passes through a short expansion die, where a temperature and pressure difference can cause product expansion. This expansion is a key attribute that appeals to consumers by enhancing the product's crispiness (Beck et al., 2017). Rehydration is often necessary before consumption or further processing of low-moisture extrudates. Research shows that the rehydration of dry matter is a complex process, with the absorption of water and the rehydration of extrudates closely related to the textural properties of low-moisture extrudates (Zhang et al., 2024).

After extrusion, low-moisture products can be dried and stored for extended periods. However, products produced through high moisture extrusion need refrigeration due to their high moisture content and have shorter shelf life. Unlike the dry extrusion method, which requires additional processing steps such as rehydration, seasoning, flavouring and colouring, high-moisture extrusion simplifies these processes (Ryu, 2020). Additionally, in low-moisture extrusion, puffing occurs through a standard die, producing an enlarged meat analogue that features numerous air cells but lacks well-defined fibrous structure. In contrast, high-moisture extrusion cooking employs an elongated cooling die, which results in texturized vegetable proteins having a fibrous texture that closely resembles real meat (Ryu, 2020). High-moisture extrusion is the most economical way for producing fibrous meat analogues, attributed to its numerous advantages: continuous processing, adaptability, compounding capability, and high-temperature short-duration technology (Diaz et al., 2022). A key element in developing fibrous structures is an elongated cooling

die connected to the final segment of the barrel. The extended cooling die helps align phase-separated proteins in the flow direction at temperatures below 100 °C, which leads to the formation of fibrous structures based on proteins (Diaz et al., 2022).

Recent advancements in high moisture extrusion technology have enhanced the taste and flavour of meat analogues made from plant proteins. These developments have also revealed the added value in terms of food nutrition provided by these food products (Xiao et al., 2022).

Although plant-based products have a great potential to address the concerns about health and environmental issues associated with meat production, the consumption of plant-based meat analogues faces several challenges (Ishaq et al., 2022). To date, there has been insufficient study on the combination of several vegetable components in the field of high-moisture meat analogue production (Lee et al., 2023b).

1.3 Plant Proteins

The plant-based meat analogues are mainly produced using powdered isolate or concentrate, which are high in terms of oligosaccharides, polyunsaturated fatty acids and dietary fibre content. Research has shown that consumption of these plant-based proteins has significantly decreased the risk of obesity and cardiovascular disease (Shaghaghian et al., 2022).

Soybean protein, with its exceptional gelation properties and ability to form a desirable fibrous matrix structure, is commonly used to create meat substitutes through extrusion processes. However, this trend is starting to shift (Lee et al., 2023a). Deforestation, as well as growing consumer awareness of the potential negative health effects of soybean protein, are significant factors driving this change (Carmo et al., 2021).

The utilization of legumes, oilseeds, and cereals from sources other than soy protein in the production of plant-based meat analogues is becoming increasingly important

in order to ensure the future sustainability of the food supply and meet consumer demands. Additionally, the use of protein-rich by-products from the food industry in the production of meat analogues would represent a significant waste reduction (Jia et al., 2021).

1.4 Hemp

Hemp (*Cannabis sativa L*) has been cultivated for thousands of years. It has been extensively cultivated for its food, medical applications, and fiber content. Hemp is a versatile crop that can thrive in a variety of climates, including both colder and warmer conditions compared to other plants grown in temperate regions like peas. With the legalization of hemp production and the recognition of its potential to yield a wide range of products, numerous industries have taken an interest in this plant (Nasrollahzadeh et al., 2022). Hemp production is widespread in Europe, Central Asia, the Philippines and China (Chen et al., 2023). High levels of unsaturated fatty acids and high protein content in hemp seeds make them suitable for processing and consumption (Leonard et al., 2022).

Hempseed is highly nutritious, with 25–35% unsaturated fatty acids, 20–25% protein, 10–15% dietary fiber, as well as various minerals and vitamins (Zahari et al., 2023). Hempseed is primarily used for oil production and oil is produced by extracting oil from hempseeds through screw pressing, which leaves behind a residue known as a meal or cake. This residue contains a protein composition primarily composed of globular globulins and albumins. The amino acid profile of these proteins complements that of other plant proteins, such as pea proteins, excellently (Nasrollahzadeh et al., 2022).

Table 1: Amino acid composition (g/100 g) of hemp protein isolate (HPI), hemp protein concentrate (HPC), soy protein isolate (SPI), red meat and chicken breast

Amino acid	HPI¹	HPC¹	SPI²	Red Meat³	Chicken Breast⁴
Alanine	4.32	4.09	3.59	1.23	1.07
Arginine	13.50	12.90	6.67	1.52	1.88
Aspartic acid	11.00	10.10	10.20	2.03	1.92
Cysteine	1.02	1.61	1.05	0.22	0.22
Glutamic acid	17.50	17.70	17.45	2.90	3.71
Glycine	4.14	4.18	3.60	0.89	0.87
Histidine	2.65	2.69	2.30	0.90	0.74
Isoleucine	3.99	3.43	4.25	0.80	0.83
Leucine	6.62	6.26	6.78	1.39	1.51
Lysine	3.08	3.45	5.33	1.78	2.12
Methionine	1.58	2.26	1.13	0.50	1.06
Phenylalanine	4.73	4.29	4.59	0.80	0.79
Proline	3.89	3.81	4.96	0.07	0.56
Serine	5.17	5.03	4.59	0.60	0.99
Threonine	3.47	3.30	3.14	0.91	1.05
Tryptophan	1.37	1.36	1.12	0.91	0.44
Tyrosine	3.76	3.55	3.22	0.91	0.66
Valine	4.97	4.35	4.10	0.88	1.02

¹Taken From Amagliani et al., 2023, ²taken from Kalman, 2014, ³taken from Alekseeva & Kolchina, 2019, ⁴taken from Dalle Zotte et al., 2020.

Lately, hemp seed has been drawing attention from consumers in the food industry. It is used in human consumption and animal feed in various forms such as whole seeds, extracted oil, press cake (a by-product of the oil extraction process), protein powder, and flour (Zahari et al., 2023).

When hemp oil is obtained from industrial hemp seeds using the cold pressing method, 35% of hemp oil and 65% of hemp press cake are obtained by weight. The hemp press cake by-product contains approximately 50% protein, 3.2% ash, and has a moisture content of 6.7%. The remaining components, amounting to 39.9%, are mainly carbohydrates. These characteristics make hemp press cake a valuable source of protein for the food production sector (Zahari et al., 2023).

In the study it is aimed to investigate the utilization of hemp flour, a by-product of oil extraction, in the production of high-protein items such as meat analogues using both low and high moisture extrusion techniques. The effect of moisture levels and temperature on the techno-functional properties of the extruded products generated by these two these two separate techniques were examined.



CHAPTER 2

MATERIALS AND METHODS

2.1 Materials

Hemp flour was purchased from Hempium Life (Amasya, Türkiye). Soy protein isolate (Vegrano) and gluten (Alfasol) were obtained from Kimbiotek Chemical Substances San. Tic. A.Ş. (İstanbul, Türkiye). The compositions of the flours were provided in Table 2, as specified by the companies. Chicken breasts (Erpiliç, Bolu, Türkiye), sunflower oil (Yudum, Balıkesir, Türkiye), soy granule (Soflex, Balıkesir, Türkiye) and soy chunk (Soflex, Balıkesir, Türkiye) were bought from supermarkets. Soy granule and soy chunk comprises 51% protein, 36% carbohydrate, 14% dietary fibre and 1% fat as indicated on the labels.

Table 2: Compositions of the flours as specified by the companies

Flours	Protein (%)	Carbohydrate (%)	Fat (%)	Dietary fibre (%)
Hemp Flour	31.7	3	8.8	51
Gluten Flour	82	8.1	1.5	-
Soy Protein Isolate	90.2	3	-	1.5

2.2 Methods

Low-moisture and high-moisture meat analogues were produced using their corresponding extrusion techniques and then analysed.

2.2.1 Low Moisture Extrusion

Laboratory scale co-rotating twin-screw extruder with computer control and data acquisition system (Feza Machine Co. Ltd., Istanbul, Türkiye) was used. The barrel length-to-diameter ratio (L:D) was 25:1, and the die diameter was 3 mm. The screw configuration of the extruder is shown in Table 3.

Table 3: Screw configurations of the extruder

8 D Twin lead feed screws

7x30° Forward kneading elements

4 D Twin lead feed screws

4x60° Forward kneading elements

4x30° Reverse kneading elements

2D Twin lead feed screws

6x60° Forward kneading elements

4x30° Reverse kneading elements

1 D Single lead feed screws

7x90° Kneading elements

2 D Single lead feed screws

Die

Screw diameter (D) = 25 mm.

One kneading element = 0.25 D.

Hemp flour (10.40% moisture) was mixed with gluten flour (8.32% moisture) to have 60:40 (g:g) hemp flour to gluten flour ratio on a dry basis. The hemp and gluten flour mixtures were extruded at three different moisture level and two different barrel temperature profiles. Moisture levels were adjusted to 20%, 30%, and 40% during extrusion using a water pump integrated into the extruder. The two distinct heating zone (and die) temperature profiles set along the extrusion direction were 60°C, 70°C, 100°C, 120°C, (die 110°C), and 60°C, 70°C, 100°C, 150°C, (die 130°C). The

flow rate of the feed was 33.33 ± 1.00 g/min, and the screw speed was 107 rpm for all samples.

Samples were collected only when the measured barrel zone and die temperatures deviated by no more than $\pm 2^\circ\text{C}$ from the set temperatures. The extrudates were allowed to cool at room temperature for 30 minutes and dried at 50°C for 24 h. Subsequently, they were stored in closed containers until analysis.

A halogen moisture analyser at 160°C (MX-50, AND, Japan) was used to determine the moisture contents.

2.2.1.1 Bulk Density

Bulk densities of the samples were measured according to the method described by Webb et al. (2020) with some modifications. A 500 mL graduated cylinder with a pre-determined mass was completely filled with the samples levelled, and then mass determined by an analytical balance. Bulk density was calculated using the Eq. (1):

$$\text{Bulk Density (g/L)} = \frac{\text{Mass of the sample}}{0.5} \quad (1)$$

2.2.1.2 Water Absorption Index (WAI) and Water Solubility Index (WSI)

The water absorption index (WAI) and water solubility index (WSI) of LMMAs and commercial soy granules and soy chunks were determined according to the method described by Webb et al., (2020) with some modifications. Samples were ground (SCM-2914, Sinbo, Türkiye) and sieved (200, Fritsch, Germany) to obtain a uniform particle size. 30 mL distilled water was mixed with 2.50 ± 0.01 g of sample in a pre-weighed 50 mL-tube and then tube was vortex mixed for 5 minutes. The tubes containing water-sample slurries were placed on a shaker (JSSB-30T, JS Research Inc., Korea) and shaken for 30 minutes at 100 rpm. After the shaking step, the tubes were centrifuged (2-16PK, Sigma, Laborzentrifugen, Germany) at $3000 \times g$ for 15

minutes. The supernatant was transferred into a pre-weighed petri dish to be dried. The tube which contains the remainder was used to determine the mass of the wet sample residual in the centrifuge tube ($m_{\text{wet residual}}$). The supernatant in the petri dish was dried at 100° C overnight until all water is evaporated. The petri dish containing the soluble dry matter in the supernatant was weighed to determine the weight of the amount of dry solid in the supernatant ($m_{\text{dry solid in supernatant}}$) by an analytical balance.

WAI and WSI of the samples were calculated using the Eq. (2) and Eq. (3) where ($m_{\text{dry sample}}$) is the amount of dry matter in 2.50±0.01 g of sample:

$$\text{WAI (g/g)} = \frac{m_{\text{wet residual}}}{m_{\text{dry sample}}} \quad (2)$$

$$\text{WSI (\%)} = \frac{m_{\text{dry solid in supernatant}}}{m_{\text{dry sample}}} \times 100 \quad (3)$$

2.2.1.3 Oil Absorption Index (OAI)

The oil absorption index (OAI) of the samples were determined using a method similar to the water absorption index method. 2.50±0.01 g of ground (SCM-2914, Sinbo, Türkiye) and sieved (200, Fritsch, Germany) sample was mixed with 30 mL sunflower oil in a pre-weighed 50 mL centrifuge tube, and then the tube was vortex mixed for 5 minutes. The tubes containing oil-sample slurries were placed on a shaker (JSSB-30T, JS Research Inc., Korea) and shaken for 30 minutes at 100 rpm. After the shaking step, the tubes were centrifuged (2-16PK, Sigma, Laborzentrifugen, Germany) at 3000xg for 15 minutes. The centrifuge tube containing oily residue in the tube was separated from the supernatant and used to determine the mass of the oily residual ($m_{\text{oily residual}}$).

OAI of the samples was calculated using the Eq. (4) where ($m_{\text{dry sample}}$) is the amount of dry matter in 2.50±0.01 g of sample:

$$\text{OAI (g/g)} = \frac{m_{\text{oily residual}}}{m_{\text{dry sample}}} \quad (4)$$

2.2.1.4 Water Holding Capacity (WHC)

Water holding capacity (WHC) of samples were determined according to the method described by Webb et al. (2020). Excess distilled water (200 mL) was added to soak 15.00 ± 0.01 g sample (m_{initial}) in a 250 mL beaker and held for 20 minutes at room temperature. Samples were drained on a mesh sieve (1000 μm , BS410/1986, Endecotts, England) for 5 minutes and weighed to determine the final mass of the wet sample (m_{final}).

WHC was calculated using the Eq. (5):

$$\text{WHC (\%)} = \frac{m_{\text{final}} - m_{\text{initial}}}{m_{\text{initial}}} \times 100 \quad (5)$$

2.2.1.5 Integrity Index

Integrity index values of samples were determined using the method described by Samard et al. (2019), with some modifications. 100 mL distilled water was added to 5.00 ± 0.01 g sample in a 250 mL beaker and placed in a water bath at 80°C (JSSB-30T, JS Research Inc., Korea) for 30 minutes. The beakers containing samples-water slurry was autoclaved (NC 90M, NUVE, Türkiye) at 121°C for 15 minutes. Tap water was spilled on samples drained on a mesh sieve (1000 μm , BS410/1986, Endecotts, England) for 30 seconds to remove tiny particles attached to the surface of the samples. Samples were transferred into a pre-weighed petri dish and dried at 100°C overnight. After drying the petri dishes containing the dry residual were used to determine the final mass of the dry sample (m_{final}).

The integrity index of the samples was calculated using the Eq. (6) where (m_{initial}) is the amount of dry matter in 5.00 ± 0.01 g sample

$$\text{Integrity Index (\%)} = \frac{(m_{\text{final}})}{(m_{\text{initial}})} \times 100 \quad (6)$$

2.2.1.6 Colour Measurements

The colour parameters, L^* (lightness), a^* (greenness-redness) and b^* (blueness-yellowness) of the samples were determined by a colour reader (CR-10, Konica Minolta, Japan). Extruded products were grinded (SCM-2914, Sinbo, Türkiye) and passed through a sieve (200, Fritsch, Germany). Then the obtained powder was flattened and compressed before the colour analyses.

2.2.1.7 Texture Profile Analyses (TPA)

Texture Profile Analysis (TPA) of LMMAs was conducted according to the method described by Lee et al. (2022b) with some modifications using a texture analyser (TA.XT Plus, Stable Micro Systems, UK). Extrudates were cut into the 10 mm in length. Each extrudate was compressed for one cycle. Hardness analysis parameters for dry LMMAs include a 30 kg load cell, a preliminary test speed of 1 mm/s, a test speed of 0.5 mm/s, a final test speed of 1 mm/s, a deformation distance of 50% strain, and a 5 g trigger force.

TPA analyses were also conducted for hydrated LMMAs. Extrudates that were cut into the 10 mm in length held in excess distilled water in a 250 mL beaker at 80°C for 30 minutes. Hydrated extrudates drained on a mesh sieve, 1000 μm (BS410/1986, Endecotts, England) for 15 minutes. Each piece with 10 mm length was compressed to 50% of its original height using SMS-P/100 \varnothing 100 mm probe in two cycles. The load cell, preliminary test speed, test speed, final test speed, deformation distance, waiting time between two cycles, and trigger force values used in the compression test were 30 kg, 1 mm/s, 0.5 mm/s, 1 mm/s, 50% strain, 5 s, and 5 g respectively.

The force-time graph (TPA profile) obtained from the force-time data were used to calculate hardness, resilience, cohesiveness, springiness, and chewiness values using

Simplified TPA Macro mode of Exponent software (Stable Micro Systems, UK) according to the equations below for the dry and hydrated samples.

$$\text{Hardness (N)} = \text{The peak force of the 1}^{\text{st}} \text{ compression curve} \quad (7)$$

$$\text{Resilience} = \frac{(\text{Area under the curve of the 1}^{\text{st}} \text{ withdrawal})}{(\text{Area under the curve of the 1}^{\text{st}} \text{ compression})} \quad (8)$$

$$\text{Cohesiveness} = \frac{(\text{Area under the 2}^{\text{nd}} \text{ compression curve})}{(\text{Area under the 1}^{\text{st}} \text{ compression curve})} \quad (9)$$

$$\text{Springiness} = \frac{(\text{Time needed to reach maximum force of the 2}^{\text{nd}} \text{ compression curve})}{(\text{Time needed to reach maximum force of the 1}^{\text{st}} \text{ compression curve})} \quad (10)$$

$$\text{Chewiness (N)} = \text{Hardness} \times \text{Cohesiveness} \times \text{Springiness} \quad (11)$$

2.2.2 High Moisture Extrusion

A long cooling die, designed for high moisture extrusion, was connected to the twin screw extruder detailed in section 2.2.1 using an adapter. The 360 mm die had three independently cooled zones, each regulated by water flow. The die maintained a consistent 7 mm high and 25 mm wide opening throughout its length.

Hemp flour (10.40 % moisture) was mixed with soy protein isolate (7.16 % moisture) to obtain three mixtures with hemp flour to soy protein isolate ratios of 0:100, 25:75, and 50:50 (g: g) on a dry basis. Each mixture was processed at three different moisture levels and two different temperature profiles. The feed moisture content was adjusted to 65 %, 70 %, and 75 % using an integrated water pump within the extruder. The two distinct heating zone temperature profiles set along the extrusion direction were 40°C, 60°C, 80°C, 100°C, and 60°C, 80°C, 100°C, 125°C. The adapter (100°C) and the cooling zone temperatures (70°C, 50°C, 40°C) were same for both extrusion temperature profiles. The feed flow rate (16.66 ± 1.00 g/min) and screw speed (215 rpm) were kept constant across all samples. Samples were

collected only when the measured barrel zone, adapter, and cooling zone temperatures deviated by no more than $\pm 2^{\circ}\text{C}$ from the set temperatures. The extrudates were allowed to cool at room temperature for 30 minutes and then stored at -20°C until analysis.

A halogen moisture analyser at 160°C (MX-50, AND, Japan) was used to determine the moisture contents.

2.2.2.1 Colour Measurements

Before taking colour measurements, high-moisture meat analogues (HMMA) were removed from the deep freezer and thawed at 4°C for one day. Subsequently, the colour parameters, L^* (lightness), a^* (greenness-redness) and b^* (blueness-yellowness) of the samples were determined by a colour reader (CR-10, Konica Minolta, Japan). For each hemp-containing sample, HMMA with the hemp flour: soy protein isolate ratio of 0:100 produced at the same temperature and moisture with the sample of interest was used as the control for the calculation of colour difference, ΔE (Eq. 12).

$$\Delta E = \sqrt{(L_{\text{sample}}^* - L_{\text{control}}^*)^2 + (a_{\text{sample}}^* - a_{\text{control}}^*)^2 + (b_{\text{sample}}^* - b_{\text{control}}^*)^2} \quad (12)$$

where L_{sample}^* , a_{sample}^* , b_{sample}^* represent the sample of interest and L_{control}^* , a_{control}^* , b_{control}^* represents the HMMA with the hemp: soy protein isolate ratio of 0:100 produced at the same temperature and moisture with the sample of interest.

2.2.2.2 Texture Profile Analyses (TPA) and Degree of Texturization

The high-moisture meat analogues (HMMA) were taken out of the deep freezer and allowed to defrost at 4°C for one day prior to analysis. Textural properties and degree of texturization were measured using a texture analyser (TA.XT Plus, Stable Micro Systems, UK). Extrudates were cut into 2.4 cm length to have the size of 2.4 x 2.4 x

0.7 cm (Length x Wide x Height). Raw and cooked chicken breasts cut into same size (2.4 x 2.4 x 0.7 cm) were also analysed for comparison. Chicken breast was cooked according to method described by Chiang et al. (2019b) with some modifications. The breast was held in a water bath (JSSB-30T, JS Research Inc., Korea) at 80°C to reach an internal temperature of 75°C and cooled at room temperature for 30 minutes before the measurements.

The samples were compressed to 50% of their original height using SMS-P/100 Ø 100 mm probe in two cycles. TPA analysis settings include a load cell with a capacity of 30 kg, a preliminary test speed of 1 mm/s, a test speed of 0.5 mm/s, a final test speed of 1 mm/s, a deformation distance of 50% strain, a waiting period of 5 seconds between two cycles, and a trigger force of 5 g. The force-time data were used to determine hardness, resilience, cohesiveness, springiness, and chewiness values using the Exponent software according to the equations below.

$$\text{Hardness (N)} = \text{The peak force of the 1}^{\text{st}} \text{ compression curve} \quad (13)$$

$$\text{Resilience} = \frac{(\text{Area under the curve of the 1}^{\text{st}} \text{ withdrawal})}{(\text{Area under the curve of the 1}^{\text{st}} \text{ compression})} \quad (14)$$

$$\text{Cohesiveness} = \frac{(\text{Area under the 2}^{\text{nd}} \text{ compression curve})}{(\text{Area under the 1}^{\text{st}} \text{ compression curve})} \quad (15)$$

$$\text{Springiness} = \frac{(\text{Time needed to reach maximum force of the 2}^{\text{nd}} \text{ compression curve})}{(\text{Time needed to reach maximum force of the 1}^{\text{st}} \text{ compression curve})} \quad (16)$$

$$\text{Chewiness (N)} = \text{Hardness} \times \text{Cohesiveness} \times \text{Springiness} \quad (17)$$

The degree of texturization was determined according to the method described by (Lee et al., 2023b). Extrudates and the chicken breast samples, with the size of 2.4 x 2.4 x 0.7 cm (Length x Wide x Height), cut into 90 % of its original height using a 60 mm wide knife edge probe (CT3-TA7, Brookfield, USA) parallel to the extrusion flow direction (longitudinal) and perpendicular to the flow direction (transversal). The cutting strength settings were as follows: load cell - 30 kg; preliminary test speed

- 1 mm/s; test speed - 0.5 mm/s; final test speed - 1 mm/s. The cutting distance is 90% strain, and the trigger force is 5 g. The degree of texturization was calculated using the formula below.

$$\text{Degree of Texturization} = \frac{(\text{Transversal cutting strength})}{(\text{Longitudinal cutting strength})} \quad (18)$$

2.2.3 Statistical Analyses

The results were analysed using analysis of variance (ANOVA). Tukey's Multiple Comparison Test was used to determine statistically significant differences between the samples ($p \leq 0.05$). Minitab 19 Statistical Software (Minitab LLC, State Collage, USA) was used for statistical analyses.

CHAPTER 3

RESULTS AND DISCUSSION

3.1.1 Low Moisture Extrusion







3.1.1.1 Physical properties

The low moisture meat analogue (LMMA) samples produced through extrusion at varying moisture levels and temperature profiles exhibited irregular shapes and lengths (Figure 1). As the extruded material exited the die, the superheated water within the melt vaporized, causing rapid expansion and moisture loss. The effect of sudden expansion of vapor was more pronounced in the samples with higher moisture level (30% and 40%), resulting in greater fragmentation (Figure 1). The irregular shapes of the LMMAs made it difficult to compare their bulk densities. On the other hand, LMMAs had a higher bulk density than commercial soy granules and commercial soy chunks (Table 4). This could be attributed to the physical properties of these products: commercial soy granules were more uniform in size compared to LMMAs, while soy chunks were larger and have a cubic shape. Additionally, commercial products undergo more intensive processing, involving higher temperatures, shear forces, and pressure due to the use of larger-scale machinery, leading to more expansion in the extrudates.

Among the LMMAs, only the samples extruded at 120°C at 30% and 40% moisture level had lower water absorption index (WAI) values, 2.57 ± 0.02 , and 2.66 ± 0.07 g/g, respectively (Table 4). The WAI quantifies the capacity of a substance to adsorb water at the macroscopic scale. Given that the extrudates were ground before the measurement, the water absorption is directly related to the level of processing and how it impacts the capacity of the macromolecular structure to accumulate or retain

water (Webb et al., 2020). As proteins denature, their water absorption increases because of the formation of a protein matrix supported by hydrophobic interactions (Webb et al., 2020). Samples with lower WAI values at 120°C may be due to low denaturation levels, resulting in a low protein matrix supported by hydrophobic interactions. Commercial soy granules and chunks exhibited a higher (no statistical analyse performed) water absorption index (WAI) than the hemp:gluten LMMAs. This disparity may be attributed to differences in protein type and processing conditions. While the exact processing conditions of commercial products are unknown, their higher WAI suggests that they undergo more intensive processing, likely involving elevated temperatures, shear forces, and pressure due to the utilization of larger-scale equipment.

Figure 1: Images of LMMA samples extruded at different moisture level and temperature profiles

Last Zone Temp.	H:G Ratio	Moisture Level		
		20%	30%	40%
120 °C	60:40			
				

H: Hemp Flour; G: Gluten Flour

Water solubility index (WSI) can vary significantly based on the specific parameters used in each extrusion operation. Factors influencing index values can be categorized into two primary groups one related to the raw material being extruded and the other related to the extruder apparatus (Oikonomou & Krokida, 2012). The first set includes parameters such as the original composition and formulation of the raw material, any pre-processing treatments, the initial particle size of the milled materials, and the milling operation (Oikonomou & Krokida, 2012). The second group refers to extruder parameters, such as extruder type, terminal barrel temperature, die temperature, feed moisture content, feed rate, screw speed, screw configuration, screw compression ratio, die dimensions, and die configuration (Oikonomou & Krokida, 2012). During the extrusion process, the physical and chemical properties of the feed components, such as protein, starch, and fibre, undergo changes. The water solubility of the extrudate is the result of the combined solubility of protein, starch, and fibre (Cheng et al., 2022). The water solubility index (WSI) values of all hemp:gluten LMMA samples were significantly lower than those of commercial soy granules and soy chunks. This indicated greater starch damage in the commercial products, likely resulting from more intense processing conditions (Table 4).

Samard and Ryu (2019b) demonstrated that the oil absorption index (OAI) is influenced by the amino acid profile, which varies across different groups with different polarities. The researchers linked the higher oil absorption index in some meat analogue samples to their elevated hydrophobic amino acid content, which could potentially bind to the hydrocarbon side chain of oil.

The OAI values of all LMMA samples were comparable to commercial soy granules and soy chunks (Table 4). Singh and Koksel (2021) found a negative correlation between surface hydrophobicity and extrusion temperature. This correlation could align with our result showing a slight rise in the oil absorption index under lower barrel temperature at higher moisture conditions. They also stated that increasing feed moisture content generally led to a better oil absorption index (Singh & Koksel, 2021).

Protein molecules unfold after being heated, exposing non-polar amino acids on the surface. This allows oil particles to bind more easily to the protein molecules through hydrophobic interactions (Singh & Koksel, 2021). According to the results (Table 4), the samples produced in this study are as desirable as the commercial products.

WHC is the parameter that indicates the quantity of water that could be bound to the LMMA structure after rehydration. The water holding capacity (WHC) significantly correlated with the porosity and dimensions of air cells in the structure (Samard & Ryu, 2019b). When samples are submerged in water, the empty spaces are filled with water. The water forms hydrogen bonds with the hydroxyl groups of the materials as it moves through the pores and capillaries (Lee et al., 2022)

Commercial soy granules exhibited significantly higher water holding capacity (WHC) than hemp:gluten LMMAs and commercial soy chunks (Table 4). The commercial soy chunk exhibits a very stiff structure with small air cells enclosed by thick walls, hindering water diffusion. LMMAs produced at 20% moisture level exhibited lower WHC than LMMAs produced at higher moisture levels (30 % and 40 %), at both temperature profiles, due to smaller pore sizes and stiff structure of the samples. The ability to hold water is an important factor in determining the texture of food. Foods with high water holding capacity lose less moisture when heated (Lee et al., 2022b). Before cooking, low-moisture meat analogues should be rehydrated in order to mimic the mouthfeel of real meat. The water holding capacity of the meat analogue is a critical factor in imitating the juiciness and chewiness of a real meat (Lee et al., 2022). In order to replicate the texture, juiciness, and chewiness of real meat, plant-based meat substitutes need to have a high-water holding capacity (Lee et al., 2022b).

The quality and yield of texturized vegetable protein are greatly affected by the integrity index, which is a crucial texture parameter. The integrity index refers to the texture characteristics of meat analogues after the pellet sample has been hydrated, pressurized and dried (Samard & Ryu, 2019a). The sample with a high integrity index indicates strong protein texturization, characterized by a robust structure that

is minimally affected by high temperature and pressure (Samard et al., 2021). An increased integrity index also indicates the formation of texture among protein molecules, resulting in reduced solid loss and improved product quality (Rajendra et al., 2023a). Integrity index of hemp:gluten LMMAs were higher than commercial soy granules (Table 4). This indicated that hemp:gluten LMMAs can stand the hydration, high temperature and pressure, similar to soy chunk, and better than commercial soy granule.



Table 4: Physical Properties of LMMAs extruded at different moisture levels and temperatures profiles

Last Zone Temp.	H:G Ratio	Moisture (%)	Bulk Density (g/L)	Water Absorption Index (g/g)	Water Solubility Index (%)	Oil Absorption Index (g/g)	Water Holding Capacity (%)	Integrity Index (%)
120 °C		20	388.45±14.55 ^{ba}	3.11±0.10 ^{aa}	9.50±0.20 ^{aa}	2.14±0.05 ^{ca}	195.53±5.39 ^{ba}	60.32±1.08 ^{bb}
		30	402.62±7.63 ^{ba}	2.57±0.02 ^{bb}	9.62±0.01 ^{aa}	2.38±0.02 ^{ba}	210.87±3.84 ^{ab}	66.29±2.54 ^{aa}
		40	479.05±6.27 ^{aa}	2.66±0.07 ^{bb}	9.41±0.23 ^{aa}	2.62±0.07 ^{aa}	218.68±5.04 ^{aa}	46.82±1.51 ^{cb}
150 °C	60:40	20	403.51±8.51 ^{aa}	2.95±0.04 ^{aa}	8.50±0.46 ^{bb}	2.21±0.07 ^{aa}	181.69±3.68 ^{bb}	71.68±1.41 ^{aa}
		30	400.52±6.78 ^{aa}	3.06±0.15 ^{aa}	10.86±1.30 ^{aa}	2.21±0.04 ^{ab}	219.82±1.87 ^{aa}	65.79±3.92 ^{aa}
		40	383.10±3.26 ^{bb}	3.17±0.04 ^{aa}	9.76±0.36 ^{abA}	2.23±0.06 ^{ab}	224.27±4.40 ^{aa}	64.34±4.59 ^{aa}
Soy Granule			331.49±3.45	3.91±0.07	20.79±0.13	2.24±0.01	373.31±11.36	37.99±1.56
Soy Chunk			215.07±4.50	3.59±0.09	22.09±0.06	2.11±0.03	165.83±17.99	64.86±2.80

H: Hemp Flour, G: Gluten Flour. Results are means ± SD (n=3). Different lower case superscripts (a,b) indicate statistical differences (p≤0.05) attributed to moisture levels in each box, while different capital superscripts (A, B) indicate statistical differences (p≤0.05) attributed to temperature profile at the same moisture in the same column.

3.1.1.2 Colour

Colour significantly influences the attractiveness and appeal of food products from a sensory perspective, as consumers often use it to gauge their appeal and desirability. Research has shown that the colour of food significantly influences purchasing decisions, as visual appeal is crucial in determining a food product's sensory quality (Landim Neves, 2024). Under high temperature, pressure, and low moisture, extrusion-cooking breaks isolates into amino acids and starch into reducing sugars through starch dextrinization (Lee et al., 2022a). The Maillard process, resulting from chemical reactions between amino acids and sugars, leads to the generation of melanoidins. The interactions among the sugars further contribute to caramelization. Additionally, oxidative decomposition of lipids and proteins can also impact colour (Caltinoglu et al., 2014). Due to these factors, the extrudates typically exhibit a darker colour compared to their source materials (Lee et al., 2022a). In our study, the L^* values of hemp:gluten LMMAs were found to be lower than those of the ingredients, in line with the suggestion of Lee et al. (2022a) (Table 5). Although the effects of moisture level and temperature during extrusion were not consistent on the colour values of the LMMAs, differing colour values after extrusion indicates interactions among the ingredients.

Table 5: Colour parameters of LMMA samples extruded at different moisture levels and temperature profiles

Last Zone Temp.	H:G	Moisture (%)	L*	a*	b*
120 °C	60:40	20	39.28±0.26 ^{cB}	0.36±0.13 ^{aB}	15.18±0.22 ^{bB}
		30	42.84±0.11 ^{bA}	- 0.14±0.11 ^{bB}	16.64±0.11 ^{aA}
		40	43.46±0.45 ^{aA}	- 0.18±0.04 ^{bB}	16.56±0.17 ^{aA}
150 °C	60:40	20	40.30±0.32 ^{aA}	0.56±0.05 ^{aA}	16.04±0.27 ^{aA}
		30	39.04±0.21 ^{bB}	0.52±0.08 ^{abA}	15.12±0.23 ^{bB}
		40	38.90±0.26 ^{bB}	0.36±0.13 ^{bA}	14.82±0.26 ^{bB}
	Hemp Flour		45.68±1.04	1.24±0.45	45.68±1.04
	Gluten Flour		73.46±1.11	0.08±1.14	73.46±1.11
	Soy Granule		56.76±0.09	1.62±0.04	56.76±0.09
	Soy Chunk		40.30±0.19	2.50±0.14	40.30±0.19

H: Hemp Flour, G: Gluten Flour. Results are means ± SD (n=5). Different lower case superscripts (a,b,c) indicate statistical differences ($p \leq 0.05$) attributed to moisture levels in each box, while different capital superscripts (A, B) indicate statistical differences ($p \leq 0.05$) attributed to temperature profile at the same moisture in the same column.

3.1.1.3 Texture Profile Analyses (TPA)

Hardness is a mechanical property that quantifies the force necessary to induce a particular deformation, penetration, or fracture of a material (Ilic et al., 2024). Generally, elevated hardness values improve consumer acceptability for meat substitutes, as their soft, mushy texture doesn't match the mouthfeel of real meat (Lee et al., 2022). On the other hand, the dietary requirements and preferences of the elderly population may be particularly well-suited to meat analogues that have lower hardness (Ghanghas et al., 2024). Resilience measures the recovery from deformation during the initial compression cycle (Soupeez et al., 2025). Cohesiveness refers to a food product's ability to retain its shape while being chewed by adhering or sticking together (Fan et al., 2024). High levels of cohesiveness and resilience suggest that the connections within the matrix are stronger. Conversely, lower cohesion and resilience result in weaker internal linkages and greater deformation (Dobson et al., 2022).

One of the most commonly used metrics from the TPA is springiness. It is calculated as the ratio of the distance to the second peak to the distance to the first peak and

relates to the elastic properties of a food item, specifically its ability to return to its original shape after being deformed (Prados et al., 2024). Chewiness refers to the mechanical texture characteristic that describes the effort required to chew a solid product until it is suitable for swallowing (Ilic et al., 2024). Meat analogues with low chewiness may be particularly beneficial for meeting the dietary needs and preferences of elderly individuals (Ghanghas et al., 2024).

Hardness (31.64 ± 12.15 N) of the hemp:gluten (H:G) sample obtained at the lower heating temperature profile (last zone temperature of 120°C) was significantly lower than the hardness of the sample (54.88 ± 16.08 N) obtained at the higher heating temperature profile (Table 6). This may be due to the higher denaturation level at 150°C compared to 120°C , which leads to greater interaction between protein molecules and results in a stiffer and harder structure.

Table 6: Hardness values of dry LMMA samples extruded at different temperature profiles

Last Zone Temperature	H:G Ratio	Hardness (N)
120 °C	60:40	31.64 ± 12.15^b
150 °C	60:40	54.88 ± 16.08^a

H: Hemp Flour, G: Gluten Flour. Results are means \pm SD (n=10). Different lower case superscripts (a,b) indicate statistical differences ($p \leq 0.05$) attributed to temperature profiles at the same H:G ratio and moisture in the same column.

The hardness and chewiness of the hydrated LMMAs were significantly higher, while resilience was lower for the samples extruded at higher heating temperature profile (Table 7). Cohesiveness and springiness were not statistically different. The increase in hardness and chewiness could be attributed to the enhanced interaction between the proteins, which leads to a firmer and more rigid structure. Similarly, integrity index results supported the TPA findings showing that the integrity index of the hydrated LMMAs significantly increased when the temperature rose to 150°C (Table 4).

Table 7: Textural properties of hydrated LMMA samples extruded at different temperature profiles

Last Zone Temperature	H:G Ratio	Moisture (%)	Hardness (N)	Resilience	Cohesiveness	Springiness	Chewiness (N)
120 °C			1.01±0.13 ^b	0.38±0.02 ^a	0.67±0.04 ^a	94.22±5.25 ^a	0.64±0.10 ^b
150 °C	60:40	20	1.64±0.41 ^a	0.35±0.02 ^b	0.68±0.05 ^a	92.23±7.40 ^a	1.01±0.26 ^a

H: Hemp Flour, G: Gluten Flour. Results are means ± SD (n=10). Different lower case superscripts (a,b) indicate statistical differences (p≤0.05) attributed to temperature profiles at the same H:G ratio and moisture in the same column

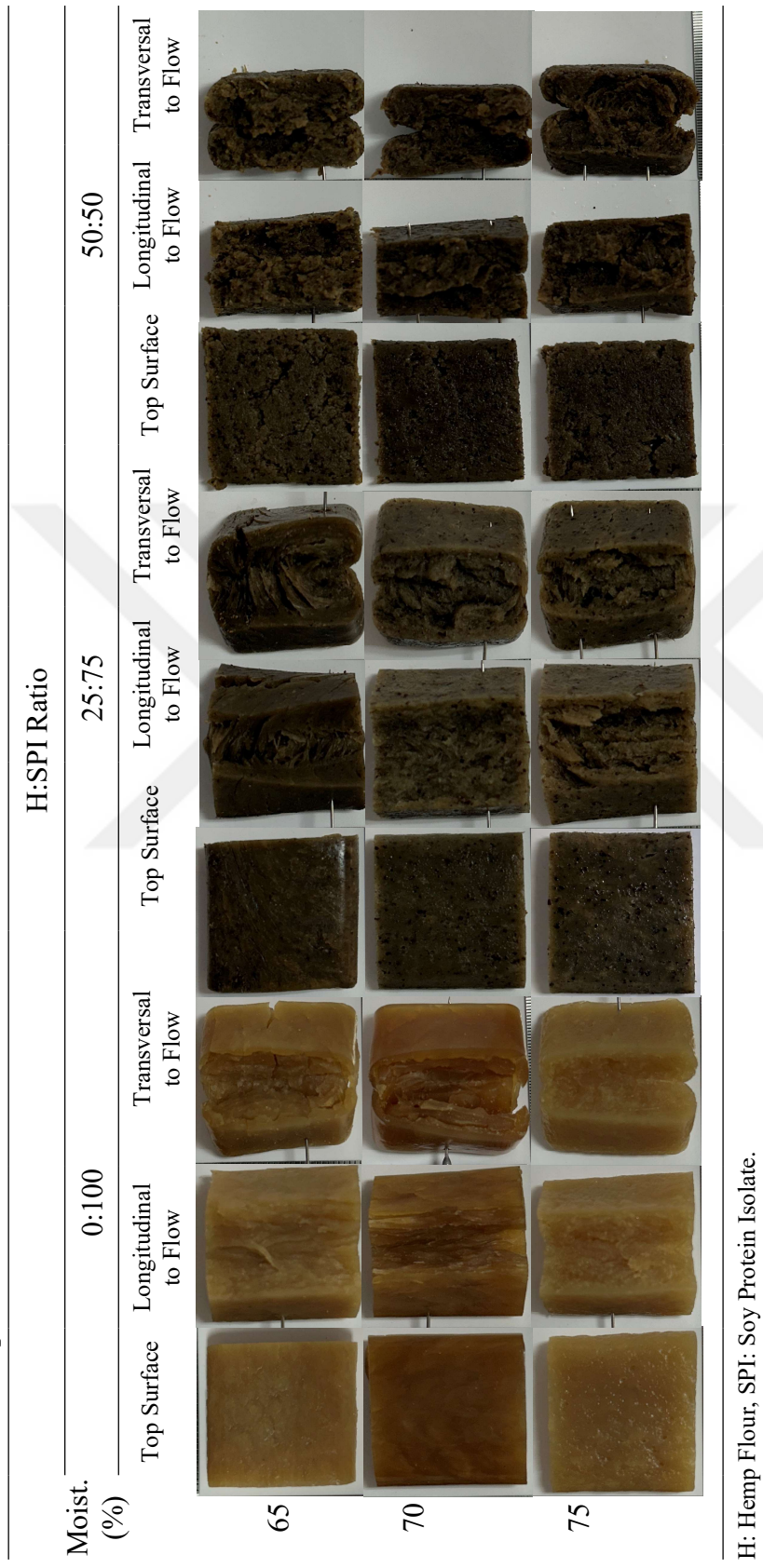
3.1.2 High Moisture Extrusion

3.1.2.1 Colour

HMMAs containing hemp flour exhibited different colour values (L^* , a^* , b^*) than control samples made only from soy protein isolate (Figure 2, Figure 3 and Table 8). The addition of hemp flour, which is darker in colour, resulted in darker (lower L^*) HMMAs. In general, increasing the extrusion temperature led to darker (lower L^*) and more bluish (lower b^*) extrudates, indicating the effect of increased Maillard reactions. However, this trend was not observed for the control SPI-only sample extruded at 75% moisture (Table 8). The overall colour difference (ΔE) between hemp-added HMMAs and their control samples decreased as the extrusion temperature was raised.


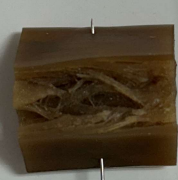















Colour is a critical aspect of food, closely linked to its quality and how consumers perceive it (Xia et al., 2023). Zahari et al. (2023) investigated the use of hempseed protein concentrate combined with oat fibre residue to manufacture meat analogues with high moisture content. Their research findings also revealed that the L^* values increased when soy protein was mixed with commercial hempseed protein concentrate (Zahari et al., 2023). Consequently, the colour of the meat analogues is expected to change depending on the protein content and additional components used.

Figure 2: Images of HMMA samples extruded at lower temperature profile (last zone temperature of 100 °C) for different moisture and hemp addition levels



H: Hemp Flour, SPI: Soy Protein Isolate.

Figure 3: Images of HMMA samples extruded at higher temperature profile (last zone temperature of 125 °C) for different moisture and hemp addition levels

Moist. (%)	H:SPI Ratio											
	0:100				25:75				50:50			
	Top Surface	Longitudinal to Flow	Transversal to Flow	Top Surface	Longitudinal to Flow	Transversal to Flow	Top Surface	Longitudinal to Flow	Transversal to Flow	Top Surface	Longitudinal to Flow	Transversal to Flow
65												
70										*	*	*
75							*	*	*	*	*	*

*The extrusion was carried out, but textured structure was not formed. H: Hemp Flour, SPI: Soy Protein Isolate.

Table 8: Colour parameters of HMMA samples extruded at different moisture and temperature profiles

Last Zone Temp.	H:SPI Ratio	Moisture (%)	L*	a*	b*	ΔE
100 °C	0:100	65	41.54±0.43 ^{aAx}	-0.02±0.16 ^{aAx}	14.76±0.19 ^{aAx}	Control
		70	40.56±0.45 ^{bAx}	-0.14±0.09 ^{aAx}	13.70±0.30 ^{bAx}	Control
		75	40.02±0.45 ^{bBx}	-1.40±0.07 ^{bBy}	12.36±0.21 ^{cBx}	Control
	25:75	65	37.26±0.09 ^{bAy}	-1.40±0.12 ^{bAy}	11.12±0.11 ^{bAz}	5.80±0.42 ^{aAx}
		70	37.10±0.16 ^{bAy}	-1.64±0.13 ^{cAz}	10.82±0.13 ^{bAy}	6.16±0.5 ^{aAy}
		75	38.50±0.37 ^{ay}	-1.10±0.10 ^{ax}	12.14±0.28 ^{ax}	1.59±0.74 ^{by}
	50:50	65	36.94±0.09 ^{aAy}	-1.10±0.07 ^{aAz}	11.70±0.07 ^{aAy}	5.64±0.32 ^{bAx}
		70	35.62±0.04 ^{cz}	-1.32±0.13 ^{by}	10.44±0.09 ^{cz}	7.45±0.37 ^{ax}
		75	35.98±0.08 ^{bz}	-1.28±0.11 ^{by}	10.70±0.12 ^{by}	4.38±0.43 ^{cx}
125 °C	0:100	65	37.72±0.31 ^{cBx}	-1.66±0.05 ^{bBx}	10.44±0.09 ^{cBx}	Control
		70	39.78±0.19 ^{bBx}	-1.08±0.08 ^{aBx}	12.58±0.08 ^{bBx}	Control
		75	42.66±0.42 ^{aA}	-0.78±0.30 ^{aA}	14.44±0.34 ^{aA}	Control
	25:75	65	35.82±0.19 ^{bBz}	-1.42±0.08 ^{aAy}	10.18±0.13 ^{bBy}	1.94±0.37 ^{bBx}
		70	36.60±0.12 ^{aBy}	-1.54±0.05 ^{bAy}	10.40±0.12 ^{aBy}	3.88±0.18 ^{aB}
		75	*	*	*	*
	50:50	65	36.52±0.13 ^{By}	-1.66±0.05 ^{By}	10.48±0.04 ^{Bx}	1.21±0.36 ^{By}
		75	*	*	*	*
		70	*	*	*	*
Hemp Flour			73.04±1.34	3.38±0.15	17.25±0.63	-
Soy Protein Isolate			45.68±1.04	1.24±0.45	20.60±0.35	-

*The extrusion was carried out, but textured structure was not formed. H: Hemp Flour, SPI: Soy Protein Isolate. Results are means ± SD (n=5). Different lower case superscripts (a,b,c) indicate statistical differences (p≤0.05) attributed to moisture levels in each box, while different capital superscripts (A, B) indicate statistical differences (p≤0.05) attributed to temperature profile at the same H:SPI ratio and moisture in the same column and different lower case superscripts (x, y, z) indicate statistical differences (p≤0.05) attributed to H:SPI ratios at the same temperature and moisture in the same column.

3.1.2.2 Texture Profile Analyses (TPA) and Degree of Texturization

Hardness is an important textural characteristic of meat analogues that are extruded at high moisture levels (Zhang et al., 2023). This measurement directly influences the chewiness and cohesiveness of meat analogues (Zhang et al., 2023). Resilience indicates the product's ability to regain its original height following compression (Zahari et al., 2020). On the other hand, "cohesiveness" refers to the product's ability to withstand a second deformation compared to its resistance to the first deformation (Mateen et al., 2023a). Cohesiveness is the main factor that influences the integrity of food products, with lower values indicating a tendency for disintegration (Soupeez et al., 2025). Springiness indicates how much a tissue distorts and recovers under external force (Yang et al., 2017). Chewiness measures the amount of effort required to chew the product to achieve a texture suitable for swallowing (Zahari et al., 2020).

In the study, in general, as the extrusion moisture levels increased, the hardness and chewiness of the samples decreased (Table 9). Only the sample obtained from the H:SPI ratio of 0:100 with 70 % moisture at 100 °C exhibited remarkably elevated values of hardness and chewiness. The moisture content of this particular sample was strikingly low during the measurements, after thawing (Table 9). It appeared to have experienced considerable loss of moisture during the frozen storage and subsequent thawing process, leading to the elevated hardness. Increasing the moisture level did not consistently affect the resilience, cohesiveness, springiness of the produced HMMAAs (Table 9).

Combining soy protein isolate with hemp flour and increasing the proportion of hemp flour from 25:75 to 50:50 reduced the hardness and chewiness of the HMMAAs produced at 70% and 75% moisture levels (Table 9). In general, increasing the heating zone temperature profiles, as indicated by the last heating zone temperatures of 100°C and 125°C, caused a reduction in the hardness values of HMMAAs. However, this trend was not observed for the control SPI-only sample extruded at 75% moisture. In general, using different hemp flour ratio and different heating

temperature profiles did not have a consistent influence on the resilience, cohesiveness, springiness and chewiness of the HMMAs.

In general, TPA values of HMMAs, especially those produced at 65% and 70% moisture levels, differed from those of raw and cooked chicken breast samples (Table 9). On the other hand, HMMAs made with hemp flour at the highest moisture level (75%) exhibited hardness and chewiness values that were closer to those of raw and cooked chicken breast (Table 9).

Extrusion factors, especially feed moisture content, can impact the textural, nutritional, sensory, and functional attributes of the end product (Rajendra et al., 2023b). The feed moisture content acts as a plasticizer and lubricant, participates in reactions, determines viscosity, aids in dough melting, and influences other system characteristics (Rajendra et al., 2023b). Decrease of hardness and chewiness with increasing moisture could be attributed to several factors, including higher moisture content, improved protein-water interaction and reduced protein aggregation (Xiao et al., 2022). As the moisture level increased, water molecules became more tightly attached to the hydrophilic binding sites on the fragmented protein chains caused by heat (Xiao et al., 2022). It is widely accepted that hardness and chewiness decrease significantly with lower protein concentration and higher moisture levels (Mateen et al., 2023b).

To measure the anisotropy of meat substitutes, the degree of texturization is determined by dividing the transverse cutting strength by the longitudinal cutting strength (Lee et al., 2023b). When the transverse cutting strength is greater than the longitudinal cutting strength, it implies the presence of a fibrous structure in the longitudinal direction, similar to that found in real meat (Lee et al., 2023b).

In the extruder barrel, the combination of shear and elevated temperature breaks down the tertiary and quaternary structures of proteins by disrupting non-covalent contacts and covalent disulfide bonds (Li et al., 2024). At the same time, new intermolecular contacts and reactions occur, resulting in the formation of a temporary protein network, where the rate of disruption of intermolecular bonds is expected to

exceed the rate of their reformation (Li et al., 2024). This leads to a decrease in bulk viscosity. The "liquefaction" phase is considered a crucial process for fibre production. Afterwards, the protein-rich mixture passes through the cooling die, solidifying due to the decreasing temperature and the increasing protein crosslink density. The formation of anisotropic structures during cooling depends on the composition of the raw material (Li et al., 2024).

The protein concentration had been shown to have a statistically significant positive impact on cutting strength in both longitudinal and transverse directions, while moisture content significantly negatively affected cutting strength both longitudinally and transversely (Mateen et al., 2023b). Water has a greater impact on textural qualities than the types of protein connections formed during extrusion. The increased water content made the products loose and soft due to insufficient texturization (Carmo et al., 2021).

A study conducted by Mazlan et al. (2020) revealed that the texturization levels of chicken breast and drumstick were 1.26 and 1.23, respectively. Several research data indicated that the degree of texturization of HMMAAs produced from soy protein, with or without additional ingredients, falls within the range of 0.7-1.7. (Mazlan et al., 2020).

In our study, increasing moisture level, heating temperature, and hemp flour addition did not consistently affect the anisotropy of the HMMAAs. The degree of texturization of HMMAAs ranged from 0.91 ± 0.08 to 1.37 ± 0.12 . In comparison, the degree of texturization of cooked chicken breast was found to be 1.72 ± 0.40 (Table 10). The results indicated that it was possible to use hemp flour up to 50:50 ratio with soy protein isolate in HMMA production.

Table 9: Textural properties of HMMA samples extruded at different moisture level and temperature profiles

Last Zone Temp. °C	H:SPI Ratio	Moisture (%)	Hardness (N)	Resilience	Cohesiveness	Springiness	Chewiness (N)	Moist. After Thawing (%)
100 °C	0:100	65	204.42±8.90 ^{bAx}	0.50±0.01 ^{bAx}	0.87±0.01 ^{aAx}	100.57±14.25 ^{aAx}	178.63±30.67 ^{bAx}	63.68±0.23
		70	374.89±18.97 ^{aAx}	0.55 ±0.01 ^{aAx}	0.86±0.01 ^{bBx}	89.87±1.65 ^{bBy}	290.19±18.25 ^{aAx}	53.96±0.24
		75	84.02±2.61 ^{cAx}	0.45±0.01 ^{cBx}	0.85±0.01 ^{cAy}	98.61±3.09 ^{aBx}	70.52±3.58 ^{cBx}	74.23±0.26
	25:75	65	208.40±7.15 ^{aAx}	0.48±0.01 ^{aAy}	0.84±0.01 ^{bAz}	90.99±2.29 ^{bBy}	158.31±6.30 ^{aBx}	60.21±0.48
		70	107.08±7.78 ^{bAy}	0.43±0.01 ^{bAy}	0.82±0.01 ^{cAz}	94.32±2.19 ^{aBx}	83.03±7.98 ^{bAy}	69.04±0.10
		75	57.57±3.26 ^{cz}	0.36±0.01 ^{cy}	0.88±0.01 ^{ax}	92.06±3.59 ^{aby}	46.78±3.85 ^{cz}	74.94±0.89
	50:50	65	182.55±8.94 ^{aAy}	0.39±0.01 ^{aAz}	0.85±0.01 ^{abAy}	93.76±1.92 ^{aAx}	145.27±8.28 ^{aAy}	60.63±0.11
		70	113.17±4.29 ^{by}	0.34±0.01 ^{bz}	0.84±0.01 ^{by}	93.08±2.54 ^{ax}	88.49±4.16 ^{by}	65.81±0.29
		75	72.74±7.21 ^{cy}	0.31±0.01 ^{cz}	0.85±0.01 ^{ay}	92.83±1.99 ^{ay}	57.53±5.94 ^{cy}	70.24±0.67
125 °C	0:100	65	162.19±9.63 ^{aBy}	0.51±0.01 ^{bAx}	0.87±0.01 ^{abAx}	116.46±30.30 ^{aAx}	163.22±42.41 ^{aAx}	64.77±0.42
		70	106.66±4.32 ^{bBx}	0.55±0.01 ^{aAx}	0.87±0.01 ^{aAx}	93.6±1.61 ^{aAy}	86.75±4.05 ^{bBx}	67.61±0.39
		75	86.21±7.28 ^{cA}	0.46±0.01 ^{cA}	0.85±0.01 ^{bA}	108.83±18.92 ^{aA}	79.70±12.47 ^{bA}	74.96±0.39
	25:75	65	187.69±14.32 ^{aBx}	0.43±0.01 ^{aBy}	0.84±0.01 ^{aAy}	126.94±31.02 ^{aAx}	201.95±61.23 ^{aAx}	61.63±0.28
		70	93.91±3.70 ^{bBy}	0.39±0.03 ^{bBy}	0.82±0.02 ^{bAy}	100.52±7.91 ^{bAx}	76.92±6.14 ^{bAy}	68.05±0.25
		75	*	*	*	*	*	*
	50:50	65	110.75±5.59 ^{Bz}	0.34±0.03 ^{Bz}	0.71±0.02 ^{Bz}	93.96±2.12 ^{Ay}	82.69±6.31 ^{By}	64.58±0.56
		70	*	*	*	*	*	*
		75	*	*	*	*	*	*
Raw Chicken Breast		58.97±11.30	0.42±0.06	0.61±0.05	89.93±8.32	32.62±9.33	-	
Cooked Chicken Breast		81.48±16.96	0.25±0.03	0.68±0.04	72.83±6.00	41.06±12.37	-	

*The extrusion was carried out, but textured structure was not formed. H: Hemp Flour, SPI: Soy Protein Isolate. Results are means ± SD (n=5). Different lower case superscripts a, b, c) indicate (statistical differences (p≤0.05) attributed to moisture levels in each box, while different capital superscripts (A, B) indicate statistical differences (p≤0.05) attributed to temperature profile at the same H:SPI ratio and moisture in the same column and different lower case superscripts (x, y, z) indicate statistical differences (p≤0.05) attributed to H:SPI ratios at the same temperature and moisture in the same column.

Table 10: Degree of texturization of HMMAAs with different H:SPI ratios produced at different moisture content and temperature profiles

Last Zone Temperature	H:SPI Ratio	Moisture (%)	Degree of Texturization F_T/F_L
100 °C	0:100	65	1.28±0.11 ^{aAx}
		70	0.98±0.08 ^{bBx}
		75	1.21±0.11 ^{aAx}
	25:75	65	1.04±0.07 ^{aAx}
		70	1.28±0.48 ^{aAx}
		75	1.19±0.10 ^{aAx}
	50:50	65	1.04±0.48 ^{ax}
		70	0.93±0.17 ^{ax}
		75	1.06±0.12 ^{ax}
125 °C	0:100	65	1.20±0.24 ^{aAx}
		70	1.37±0.12 ^{aAx}
		75	0.91±0.08 ^{bB}
	25:75	65	1.02±0.08 ^{bAx}
		70	1.26±0.21 ^{aAx}
		75	*
	50:50	65	1.23±0.19 ^{Ax}
		70	*
		75	*
Cooked Chicken Breast			1.72±0.40

*The extrusion was carried out, but textured structure was not formed. H: Hemp Flour, SPI: Soy Protein Isolate. Results are means ± SD (n=5). Different lower case superscripts (a,b,c) indicate statistical differences ($p \leq 0.05$) attributed to moisture levels in each box, while different capital superscripts (A, B) indicate statistical differences ($p \leq 0.05$) attributed to temperature profile at the same H:SPI ratio and moisture in the same column and different lower case superscripts (x, y, z) indicate statistical differences ($p \leq 0.05$) attributed to H:SPI ratios at the same temperature and moisture in the same column.



CHAPTER 4

CONCLUSION AND RECOMMENDATIONS

The research examined the physical characteristics of low moisture meat analogues (LMMAs) and high moisture meat analogues (HMMAs) produced by combining hemp flour, a by-product of oil extraction, with protein sources such as gluten and soy protein isolate respectively. The results revealed that LMMAs could be successfully produced using a 60:40 ratio of hemp flour to gluten flour. Further, the findings emphasized the feasibility of producing high-quality fibrous HMMAs that mimic the textural attributes of chicken breast by incorporating hemp flour into soy protein isolate up to 50:50 ratio.

In conclusion, the research highlights the potential of hemp flour as a valuable protein source for the development of innovative extruded products. The insights gained from this research will help food producers develop new meat analogues. Future research may focus on sensory properties to develop consumer-acceptable meat analogues made with hemp flour.



REFERENCES

- Alekseeva, E., & Kolchina, V. (2019). Amino acid composition of beef obtained from the specialized meat cattle. *IOP Conference Series: Earth and Environmental Science*, 341(1). <https://doi.org/10.1088/1755-1315/341/1/012136>
- Amagliani, L., Fanesi, B., de Oliveira Reis, G., Bovay, C., Affolter, M., & Schmitt, C. (2023). High moisture extrusion processing of hemp protein ingredients as influenced by their composition and physicochemical properties. *Science Talks*, 8, 100250. <https://doi.org/10.1016/j.sctalk.2023.100250>
- Beck, S. M., Knoerzer, K., & Arcot, J. (2017). Effect of low moisture extrusion on a pea protein isolate's expansion, solubility, molecular weight distribution and secondary structure as determined by Fourier Transform Infrared Spectroscopy (FTIR). *Journal of Food Engineering*, 214, 166–174. <https://doi.org/10.1016/j.jfoodeng.2017.06.037>
- Bolívar-Prados, M., Baixauli, R., Ismael-Mohammed, K., Ortega, O., Clavé, P., & Laguna, L. (2024). Texture-modified foods for patients with swallowing and/or mastication impairments. In *A Multidisciplinary Approach to Managing Swallowing Dysfunction in Older People* (pp. 223–231). Elsevier. <https://doi.org/10.1016/B978-0-323-91686-8.00017-3>
- Caltinoglu, C., Tonyali, B., & Sensoy, I. (2014). Effects of tomato pulp addition on the extrudate quality parameters and effects of extrusion on the functional parameters of the extrudates. *International Journal of Food Science and Technology*, 49(2), 587–594. <https://doi.org/10.1111/ijfs.12341>
- Chen, H., Xu, B., Wang, Y., Li, W., He, D., Zhang, Y., Zhang, X., & Xing, X. (2023). Emerging natural hemp seed proteins and their functions for nutraceutical applications. In *Food Science and Human Wellness* (Vol. 12, Issue 4, pp. 929–941). KeAi Communications Co. <https://doi.org/10.1016/j.fshw.2022.10.016>

- Cheng, H., Wang, H., Ma, S., Xue, M., Li, J., & Yang, J. (2022). Development of a water solubility model of extruded feeds by utilizing a starch gelatinization model. *International Journal of Food Properties*, 25(1), 463–476.
<https://doi.org/10.1080/10942912.2022.2046055>
- Chiang, J. H., Loveday, S. M., Hardacre, A. K., & Parker, M. E. (2019). Effects of soy protein to wheat gluten ratio on the physicochemical properties of extruded meat analogues. *Food Structure*, 19.
<https://doi.org/10.1016/j.foostr.2018.11.002>
- Dalle Zotte, A., Ricci, R., Cullere, M., Serva, L., Tenti, S., & Marchesini, G. (2020). Research Note: Effect of chicken genotype and white striping–wooden breast condition on breast meat proximate composition and amino acid profile. *Poultry Science*, 99(3), 1797–1803. <https://doi.org/10.1016/j.psj.2019.10.066>
- Dobson, S., Laredo, T., & Marangoni, A. G. (2022). Particle filled protein-starch composites as the basis for plant-based meat analogues. *Current Research in Food Science*, 5, 892–903. <https://doi.org/10.1016/j.crfs.2022.05.006>
- Fan, Y., Zheng, S., Annamalai, P. K., Bhandari, B., & Prakash, S. (2024). Enhancement of the texture and microstructure of faba bean-based meat analogues with brewers' spent grain through enzymatic treatments. *Sustainable Food Technology*, 2(3), 826–836.
<https://doi.org/10.1039/d4fb00045e>
- Ghanghas, N., Nadimi, M., Paliwal, J., & Koksel, F. (2024). Gas-assisted high-moisture extrusion of soy-based meat analogues: Impacts of nitrogen pressure and cooling die temperature on density, texture and microstructure. *Innovative Food Science and Emerging Technologies*, 92.
<https://doi.org/10.1016/j.ifset.2023.103557>
- Herz, E., Herz, L., Dreher, J., Gibis, M., Ray, J., Pibarot, P., Schmitt, C., & Weiss, J. (2021). Influencing factors on the ability to assemble a complex meat

analogue using a soy-protein-binder. *Innovative Food Science and Emerging Technologies*, 73. <https://doi.org/10.1016/j.ifset.2021.102806>

Ilic, J., Van den Berg, M., & Oosterlinck, F. (2024). The textural and sensory properties of plant-based meat. In *Handbook of Plant-Based Meat Analogs: Innovation, Technology and Quality* (pp. 331–346). Elsevier. <https://doi.org/10.1016/B978-0-443-21846-0.00008-3>

Ishaq, A., Irfan, S., Sameen, A., & Khalid, N. (2022). Plant-based meat analogs: A review with reference to formulation and gastrointestinal fate. In *Current Research in Food Science* (Vol. 5, pp. 973–983). Elsevier B.V. <https://doi.org/10.1016/j.crfs.2022.06.001>

Jia, W., Curubeto, N., Rodríguez-Alonso, E., Keppler, J. K., & van der Goot, A. J. (2021). Rapeseed protein concentrate as a potential ingredient for meat analogues. *Innovative Food Science and Emerging Technologies*, 72. <https://doi.org/10.1016/j.ifset.2021.102758>

Kalman, D. S. (2014). Amino acid composition of an organic brown rice protein concentrate and isolate compared to soy and whey concentrates and isolates. *Foods*, 3(3), 394–402. <https://doi.org/10.3390/foods3030394>

Landim Neves, M. I. (2024). Color solutions in plant-based foods. In *Handbook of Plant-Based Food and Drinks Design* (pp. 319–334). Elsevier. <https://doi.org/10.1016/B978-0-443-16017-2.00025-5>

Lee, J. S., Choi, I., & Han, J. (2022). Construction of rice protein-based meat analogues by extruding process: Effect of substitution of soy protein with rice protein on dynamic energy, appearance, physicochemical, and textural properties of meat analogues. *Food Research International*, 161. <https://doi.org/10.1016/j.foodres.2022.111840>

Lee, J. S., Kim, S., Jeong, Y. J., Choi, I., & Han, J. (2023a). Impact of interactions between soy and pea proteins on quality characteristics of high-moisture meat

- analogues prepared via extrusion cooking process. *Food Hydrocolloids*, 139. <https://doi.org/10.1016/j.foodhyd.2023.108567>
- Lee, J. S., Kim, S., Jeong, Y. J., Choi, I., & Han, J. (2023b). Impact of interactions between soy and pea proteins on quality characteristics of high-moisture meat analogues prepared via extrusion cooking process. *Food Hydrocolloids*, 139. <https://doi.org/10.1016/j.foodhyd.2023.108567>
- Lee, J. S., Oh, H., Choi, I., Yoon, C. S., & Han, J. (2022a). Physico-chemical characteristics of rice protein-based novel textured vegetable proteins as meat analogues produced by low-moisture extrusion cooking technology. *LWT*, 157. <https://doi.org/10.1016/j.lwt.2021.113056>
- Lee, J. S., Oh, H., Choi, I., Yoon, C. S., & Han, J. (2022b). Physico-chemical characteristics of rice protein-based novel textured vegetable proteins as meat analogues produced by low-moisture extrusion cooking technology. *LWT*, 157. <https://doi.org/10.1016/j.lwt.2021.113056>
- Leonard, W., Zhang, P., Ying, D., Nie, S., Liu, S., & Fang, Z. (2022). Post-extrusion physical properties, techno-functionality and microbiota-modulating potential of hempseed (*Cannabis sativa* L.) hull fiber. *Food Hydrocolloids*, 131. <https://doi.org/10.1016/j.foodhyd.2022.107836>
- Li, J., Janssen, F., Verfaillie, D., Brijs, K., Delcour, J. A., Gunes, D. Z., Cardinaels, R., Van Royen, G., & Wouters, A. G. B. (2024). The interplay between soy proteins and dietary fiber in determining the structure and texture of high moisture extrudates. *Food Hydrocolloids*, 156. <https://doi.org/10.1016/j.foodhyd.2024.110256>
- Mateen, A., Mathpati, M., & Singh, G. (2023a). A study on high moisture extrusion for making whole cut meat analogue: Characterization of system, process and product parameters. *Innovative Food Science and Emerging Technologies*, 85. <https://doi.org/10.1016/j.ifset.2023.103315>

- Mateen, A., Mathpati, M., & Singh, G. (2023b). A study on high moisture extrusion for making whole cut meat analogue: Characterization of system, process and product parameters. *Innovative Food Science and Emerging Technologies*, 85. <https://doi.org/10.1016/j.ifset.2023.103315>
- Mazlan, M. M., Talib, R. A., Chin, N. L., Shukri, R., Taip, F. S., Nor, M. Z. M., & Abdullah, N. (2020). Physical and microstructure properties of oyster mushroom-soy protein meat analog via single-screw extrusion. *Foods*, 9(8). <https://doi.org/10.3390/foods9081023>
- Nasrollahzadeh, F., Roman, L., Swaraj, V. J. S., Ragavan, K. V., Vidal, N. P., Dutcher, J. R., & Martinez, M. M. (2022). Hemp (*Cannabis sativa* L.) protein concentrates from wet and dry industrial fractionation: Molecular properties, nutritional composition, and anisotropic structuring. *Food Hydrocolloids*, 131. <https://doi.org/10.1016/j.foodhyd.2022.107755>
- Norajit, K., Gu, B. J., & Ryu, G. H. (2011). Effects of the addition of hemp powder on the physicochemical properties and energy bar qualities of extruded rice. *Food Chemistry*, 129(4), 1919–1925. <https://doi.org/10.1016/j.foodchem.2011.06.002>
- Oikonomou, N. A., & Krokida, M. K. (2012). Water absorption index and water solubility index prediction for extruded food products. *International Journal of Food Properties*, 15(1), 157–168. <https://doi.org/10.1080/10942911003754718>
- Prabha, K., Ghosh, P., S, A., Joseph, R. M., Krishnan, R., Rana, S. S., & Pradhan, R. C. (2021). Recent development, challenges, and prospects of extrusion technology. In *Future Foods* (Vol. 3). Elsevier B.V. <https://doi.org/10.1016/j.fufo.2021.100019>
- Rajendra, A., Ying, D., Warner, R. D., Ha, M., & Fang, Z. (2023a). Effect of Extrusion on the Functional, Textural and Colour Characteristics of

- Texturized Hempseed Protein. *Food and Bioprocess Technology*, 16(1), 98–110. <https://doi.org/10.1007/s11947-022-02923-z>
- Rajendra, A., Ying, D., Warner, R. D., Ha, M., & Fang, Z. (2023b). Effect of Extrusion on the Functional, Textural and Colour Characteristics of Texturized Hempseed Protein. *Food and Bioprocess Technology*, 16(1), 98–110. <https://doi.org/10.1007/s11947-022-02923-z>
- Ramos Diaz, J. M., Kantanen, K., Edelmann, J. M., Suhonen, H., Sontag-Strohm, T., Jouppila, K., & Piironen, V. (2022). Fibrous meat analogues containing oat fiber concentrate and pea protein isolate: Mechanical and physicochemical characterization. *Innovative Food Science and Emerging Technologies*, 77. <https://doi.org/10.1016/j.ifset.2022.102954>
- Ryu, G.-H. (2020). Extrusion cooking of high-moisture meat analogues. In *Extrusion Cooking* (pp. 205–224). Elsevier. <https://doi.org/10.1016/b978-0-12-815360-4.00007-9>
- Saldanha do Carmo, C., Knutsen, S. H., Malizia, G., Dessev, T., Geny, A., Zobel, H., Myhrer, K. S., Varela, P., & Sahlstrøm, S. (2021). Meat analogues from a faba bean concentrate can be generated by high moisture extrusion. *Future Foods*, 3. <https://doi.org/10.1016/j.fufo.2021.100014>
- Samard, S., Maung, T. T., Gu, B. Y., Kim, M. H., & Ryu, G. H. (2021). Influences of extrusion parameters on physicochemical properties of textured vegetable proteins and its meatless burger patty. *Food Science and Biotechnology*, 30(3), 395–403. <https://doi.org/10.1007/s10068-021-00879-y>
- Samard, S., & Ryu, G. H. (2019a). A comparison of physicochemical characteristics, texture, and structure of meat analogue and meats. *Journal of the Science of Food and Agriculture*, 99(6), 2708–2715. <https://doi.org/10.1002/jsfa.9438>

- Samard, S., & Ryu, G. H. (2019b). Physicochemical and functional characteristics of plant protein-based meat analogs. *Journal of Food Processing and Preservation*, 43(10). <https://doi.org/10.1111/jfpp.14123>
- Shaghaghian, S., McClements, D. J., Khalesi, M., Garcia-Vaquero, M., & Mirzapour-Kouhdasht, A. (2022). Digestibility and bioavailability of plant-based proteins intended for use in meat analogues: A review. In *Trends in Food Science and Technology* (Vol. 129, pp. 646–656). Elsevier Ltd. <https://doi.org/10.1016/j.tifs.2022.11.016>
- Shanmugam, K., Bryngelsson, S., Östergren, K., & Hallström, E. (2023). Climate Impact of Plant-based Meat Analogues: A Review of Life Cycle Assessments. In *Sustainable Production and Consumption* (Vol. 36, pp. 328–337). Elsevier B.V. <https://doi.org/10.1016/j.spc.2023.01.014>
- Singh, R., & Koksel, F. (2021). Effects of particle size distribution and processing conditions on the techno-functional properties of extruded soybean meal. *LWT*, 152. <https://doi.org/10.1016/j.lwt.2021.112321>
- Soupeze, J. B. R. G., Dages, B. A. S., Pavar, G. S., Fabian, J., Thomas, J. M., & Theodosiou, E. (2025). Mechanical properties and texture profile analysis of beef burgers and plant-based analogues. *Journal of Food Engineering*, 385. <https://doi.org/10.1016/j.jfoodeng.2024.112259>
- Sun, C., Ge, J., He, J., Gan, R., & Fang, Y. (2021). Processing, Quality, Safety, and Acceptance of Meat Analogue Products. In *Engineering* (Vol. 7, Issue 5, pp. 674–678). Elsevier Ltd. <https://doi.org/10.1016/j.eng.2020.10.011>
- Taghian Dinani, S., Allaire, N., Boom, R., & van der Goot, A. J. (2023). Influence of processing temperature on quality attributes of meat analogues fortified with L-cysteine. *Food Hydrocolloids*, 137. <https://doi.org/10.1016/j.foodhyd.2022.108422>
- Taghian Dinani, S., van der Harst, J. P., Boom, R., & van der Goot, A. J. (2023). Effect of L-cysteine and L-ascorbic acid addition on properties of meat

- analogues. *Food Hydrocolloids*, 134.
<https://doi.org/10.1016/j.foodhyd.2022.108059>
- Webb, D., Li, Y., & Alavi, S. (2023). Chemical and physicochemical features of common plant proteins and their extrudates for use in plant-based meat. In *Trends in Food Science and Technology* (Vol. 131, pp. 129–138). Elsevier Ltd. <https://doi.org/10.1016/j.tifs.2022.11.006>
- Webb, D., Plattner, B. J., Donald, E., Funk, D., Plattner, B. S., & Alavi, S. (2020). Role of chickpea flour in texturization of extruded pea protein. *Journal of Food Science*, 85(12), 4180–4187. <https://doi.org/10.1111/1750-3841.15531>
- Xia, S., Shen, S., Song, J., Li, K., Qin, X., Jiang, X., Xue, C., & Xue, Y. (2023). Physicochemical and structural properties of meat analogues from yeast and soy protein prepared via high-moisture extrusion. *Food Chemistry*, 402.
<https://doi.org/10.1016/j.foodchem.2022.134265>
- Xiao, Z., Jiang, R., Huo, J., Wang, H., Li, H., Su, S., Gao, Y., & Duan, Y. (2022). Rice bran meat analogs: Relationship between extrusion parameters, apparent properties and secondary structures. *LWT*, 163.
<https://doi.org/10.1016/j.lwt.2022.113535>
- Yang, S., He, Y., Yan, Y., Xie, N., Song, Y., Yan, X., & Ding, Z. (2017). Textural properties of stinky mandarin fish (*Siniperca chuatsi*) during fermentation: effects of the state of moisture. *International Journal of Food Properties*, 20, 1530–1538. <https://doi.org/10.1080/10942912.2016.1233433>
- Zahari, I., Ferawati, F., Helstad, A., Ahlström, C., Östbring, K., Rayner, M., & Purhagen, J. K. (2020). Development of high-moisture meat analogues with hemp and soy protein using extrusion cooking. *Foods*, 9(6).
<https://doi.org/10.3390/foods9060772>
- Zahari, I., Purhagen, J. K., Rayner, M., Ahlström, C., Helstad, A., Landers, M., Müller, J., Eriksson, J., & Östbring, K. (2023). Extrusion of high-moisture meat analogues from hempseed protein concentrate and oat fibre residue.

Journal of Food Engineering, 354.

<https://doi.org/10.1016/j.jfoodeng.2023.111567>

Zahari, I., Rinaldi, S., Ahlstrom, C., Östbring, K., Rayner, M., & Purhagen, J. (2023). High moisture meat analogues from hemp – The effect of co-extrusion with wheat gluten and chickpea proteins on the textural properties and sensorial attributes. *LWT*, 189. <https://doi.org/10.1016/j.lwt.2023.115494>

Zhang, Y., Shao, F., Wan, X., Zhang, H., Cai, M., Hu, K., & Duan, Y. (2024). Effects of rapeseed protein addition on soybean protein-based textured protein produced by low-moisture extrusion: Changes in physicochemical attributes, structural properties and barrel flow behaviors. *Food Hydrocolloids*, 149. <https://doi.org/10.1016/j.foodhyd.2023.109631>



APPENDICES

A. Moisture data of HMMA samples.

Table A: Moisture data of HMMA samples

Last Zone Temperature	H:SPI	Calculated Moisture (%)	Moisture After Extrusion (%)	Moisture After Thawing (%)
100 °C	0:100	65	63.25±0.01	63.68±0.23
		70	59.92±1.28	53.96±0.24
		75	75.27±0.01	74.23±0.26
	25:75	65	59.80±0.01	60.21±0.48
		70	73.43±0.01	69.04±0.10
		75	72.51±0.01	74.94±0.89
	50:50	65	60.52±0.50	60.63±0.11
		70	67.56±0.36	65.81±0.29
		75	71.18±0.36	70.24±0.67
125 °C	0:100	65	66.93±0.02	64.77±0.42
		70	68.26±0.03	67.61±0.39
		75	74.61±0.01	74.96±0.39
	25:75	65	61.02±0.02	61.63±0.28
		70	71.54±0.14	68.05±0.25
		75	*	*
	50:50	65	66.62±0.05	64.58±0.56
		70	*	*
		75	*	*

*The extrusion was carried out, but textured structure was not formed.

B. Images of LMMA extrudates



Figure 4: LMMA, H:G_60:40, 20% moisture, 120°C



Figure 5: LMMA, H:G_60:40, 20% moisture, 150°C

C. Images of HMMA extrudates



Figure 6: HMMA, H:SPI_0:100, 65% moisture, 100°C. Images of surface, longitudinal to flow and transversal to flow, respectively



Figure 7: HMMA, H:SPI_0:100, 70% moisture, 100°C. Images of surface, longitudinal to flow and transversal to flow, respectively



Figure 8: HMMA, H:SPI_0:100, 75% moisture, 100°C. Images of surface, longitudinal to flow and transversal to flow, respectively



Figure 9: HMMA, H:SPI_25:75, 65% moisture, 100°C. Images of surface, longitudinal to flow and transversal to flow, respectively



Figure 10: HMMA, H:SPI_25:75, 70% moisture, 100°C. Images of surface, longitudinal to flow and transversal to flow, respectively



Figure 11: HMMA, H:SPI_25:75, 75% moisture, 100°C. Images of surface, longitudinal to flow and transversal to flow, respectively

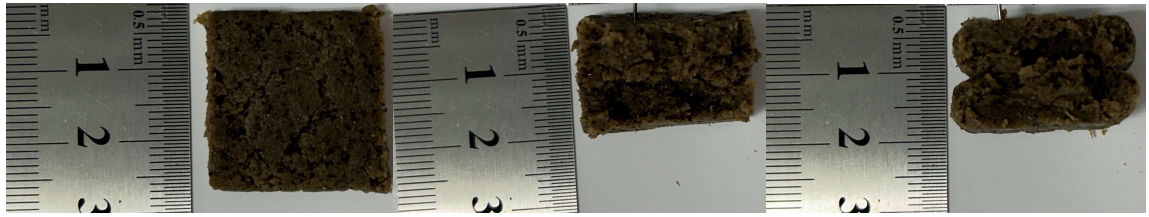


Figure 12: HMMA, H:SPI_50:50, 65% moisture, 100°C. Images of surface, longitudinal to flow and transversal to flow, respectively



Figure 13: HMMA, H:SPI_50:50, 70% moisture, 100°C. Images of surface, longitudinal to flow and transversal to flow, respectively



Figure 14: HMMA, H:SPI_50:50, 75% moisture, 100°C. Images of surface, longitudinal to flow and transversal to flow, respectively

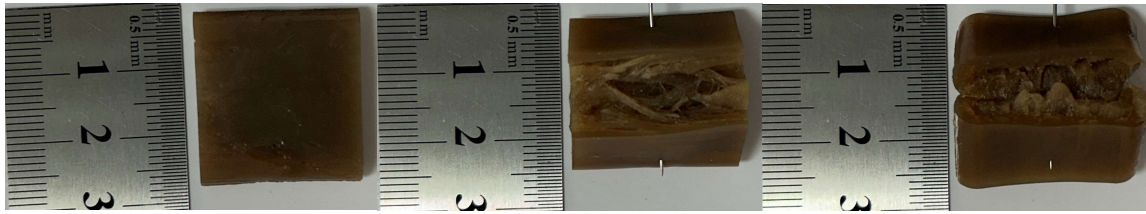


Figure 15: HMMA, H:SPI_0:100, 65% moisture, 125°C. Images of surface, longitudinal to flow and transversal to flow, respectively



Figure 16: HMMA, H:SPI_0:100, 70% moisture, 125°C. Images of surface, longitudinal to flow and transversal to flow, respectively

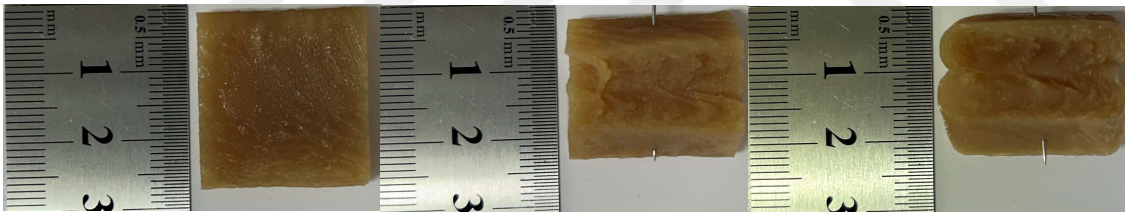


Figure 17: HMMA, H:SPI_0:100, 75% moisture, 125°C. Images of surface, longitudinal to flow and transversal to flow, respectively



Figure 18: HMMA, H:SPI_25:75, 65% moisture, 125°C. Images of surface, longitudinal to flow and transversal to flow, respectively



Figure 19: HMMA, H:SPI_25:75, 70% moisture, 125°C. Images of surface, longitudinal to flow and transversal to flow, respectively

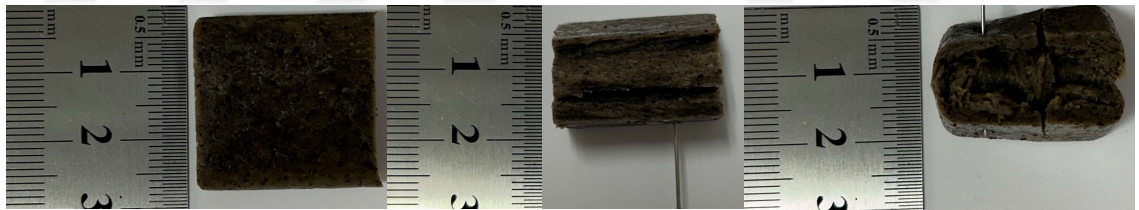


Figure 20: HMMA, H:SPI_50:50, 65% moisture, 125°C. Images of surface, longitudinal to flow and transversal to flow, respectively